

Finite temperature Aging Holography

Seungjoon Hyun¹, Jaehoon Jeong¹ and Bom Soo Kim^{2,3}

¹*Department of Physics, College of Science, Yonsei University, Seoul 120-749, Korea*

²*Crete Center for Theoretical Physics, University of Crete, Crete, Greece*

³*IESL - FORTH, P.O.Box 1527, 71110 Heraklion, Crete, Greece*

sjhyun@yonsei.ac.kr, j.jeong@yonsei.ac.kr, bskim@physics.uoc.gr

Abstract

We construct the gravity background which describes the dual field theory with aging invariance. We choose the decay modes of the bulk scalar field in the internal spectator direction to obtain the dissipative behavior of the boundary correlation functions of the dual scalar fields. In particular, the two-time correlation function at zero temperature has the characteristic features of the aging system: power law decay, broken time translation and dynamical scaling. We also construct the black hole backgrounds with asymptotic aging invariance. We extensively study characteristic behavior of the finite temperature two-point correlation function via analytic and numerical methods.

Contents

1	Introduction	2
2	Zero Temperature Aging Holography	4
2.1	Zero Temperature Aging Background : A Review	5
2.2	Aging in Light-Cone	6
2.3	Two-point Correlation Function	8
2.3.1	$M = M_R$	11
2.3.2	$M = iM_I$	12
2.4	Two-time Correlators	14
2.5	Comments on Schrödinger Background	15
2.6	Comments on Dual Field Theory	16
3	Finite Temperature Aging Holography	17
3.1	Equation of Motion	18
3.2	Finite Temperature Correlation Functions	19
3.2.1	General Features	20
3.2.2	Analytic Approaches	21
3.2.3	High Temperature Correlation Functions	22
3.2.4	Low Temperature Correlation Functions	23
3.3	Numerical Results	24
3.3.1	Description in terms of ω and k	25
3.3.2	Description in terms of \mathbf{q} and \mathbf{w}	26
3.4	Comments on Schrödinger Background	28
4	Conclusion and Outlook	30
A	High Temperature Correlator : Next Order	32
B	Series Solutions with $m = 0$	33

1 Introduction

AdS/CFT correspondence has been successful in describing strongly-coupled field theories using weakly-coupled classical gravity backgrounds, providing new paradigm of analytical methods for theories with strong coupling [1][2]. Recently this correspondence extended its application to non-relativistic setup with general dynamical exponent $z \neq 1$. Those non-relativistic holographic theories include Schrödinger [3, 4, 5, 6] and Lifshitz holography [7].¹ Since then, they have been enjoying continuous attractions.

An acquaintance of non-relativistic holographic theories with $z \neq 1$ tells that we can construct a plethora of explicit time dependent backgrounds by utilizing the distinguished role of time. This is different from the relativistic theories. Thus we might hope to shed lights on time dependent backgrounds in string theory and in AdS/CFT correspondence even though they are in general known to be challenging. We would like to add some contributions to this direction in the context of the non-relativistic Schrödinger holography with $z=2$.

One of the simplest applications of the non-equilibrium physics is known as *aging*. Aging phenomena can be characterized by two-time correlation functions, which typically show that older systems relax in a slower manner than younger systems after entering a given physical phase under study, see *e.g.* [9][10] for reviews. Two pioneering works of aging in holographic setup have been put forward in [11][12] by generalizing Schrödinger background [3][4] with explicit time dependent terms. The authors of [12] observe that aging algebra can be realized as a subset of Schrödinger algebra using a singular time dependent coordinate transformation. See also [13] for similar observations of general time dependent deformations of Schrödinger backgrounds.

Along the line of Schrödinger backgrounds [3][4], there have been progresses with much interest. Their finite temperature generalizations with the thermodynamic analysis can be found in [14, 15, 16, 17] and transport properties are analyzed in [18], recently. These solutions are constructed nicely using the null Melvin twist [19][20]. There also have been efforts constructing Schrödinger solutions from string or M theory, sometimes with supersymmetry. See [21, 22, 23, 24, 25], for example. While these Schrödinger backgrounds have been drawn much interest, the progresses directly along this line have been hindered due to the conceptual difficulties related to their non-trivial boundary structures. Furthermore

¹See *e.g.* [8] for a very different usage of the Lifshitz symmetry with $z=3$ in the context of quantum field theory of gravity.

one quickly finds that finite temperature generalizations of the Schrödinger backgrounds are complicated, and thus practical calculations are difficult.

An alternative candidate for the Schrödinger holography, AdS in light-cone, has been constructed in [5][6] even before the finite temperature generalizations of the Schrödinger backgrounds. Its finite temperature generalizations were done in [15][26] with thermodynamic analysis, and transport properties are also analyzed in [26][27]. It turns out that these two different holographic theories, Schrödinger backgrounds and AdS in light-cone, have the same thermodynamic properties [15][26] and also the same transport properties when the comparisons are reliable [26]. Thus AdS in light-cone is a viable candidate for Schrödinger holography. While it remains as a question whether these two theories describe the same physical properties or not, AdS in light-cone has advantages over the Schrödinger backgrounds: it has well-defined holographic renormalization and is as simple as original AdS in its computations.

Motivated by these observations, we would like to construct a holographic model of aging in the context of [5][6], Aging in light-cone, by realizing the aging symmetry with the singular time dependent coordinate transformation. This is done in section 2. From the bulk gravity side, we obtain the two-point correlation function of the dual field theory. In particular, we consider the, so-called, spectator coordinate x^- as an *internal* direction.² Furthermore, since we are dealing with time dependent and dissipative system, we choose the decay modes of the bulk scalar field in the internal spectator direction. This is in contrast with the complexification of spacetime done in [12]. As a result, we obtain generalized two-time correlation function of the dual field theory, which exhibit the characteristic features of the aging system.

In section 3 we consider finite temperature generalizations of the aging holography on Aging in light-cone as well as Aging in Schrödinger backgrounds. We focus on the former case, which has simpler form, and then give some comments on the latter. We study the finite temperature two-point correlation function in Aging in light-cone via AdS/CFT correspondence. We provide the novel time dependent structure of aging two-point correlation

² Note that the geometric realizations of Schrödinger symmetry separates itself from the other holographic examples, providing a correspondence between $(d, 1)$ -dimensional field theory and $(d+3)$ -dimensional gravity theory. In addition to the usual radial direction, it has another coordinate x^- , which does not contribute to the coordinates in field theory. The x^- coordinate is known to provide a non-relativistic particle number or mass, referred here by M . We call this spectator direction, x^- , as *internal* because it does not show up explicitly in the dual field theory.

While the full potential associated with the x^- direction remains to be seen, we believe that the treatment adapted in this paper is one of the first non-trivial examples of utilizing this spectator direction. See *e.g.* [28][29] for different attempts on this issue.

function in coordinate space, compared to that of Schrödinger case and to that of momentum space. As the latter is not exactly solvable, we use numerical as well as analytic methods to see its behavior. Finally, we give some comments on the aging phenomena from the Schrödinger background stressing the difference compared to those of the Aging in light-cone. It turns out that the internal isometry direction plays a crucial role throughout in this paper. In section 4, we give conclusion.

2 Zero Temperature Aging Holography

In this section, we start with a brief review of aging holography based on recent papers [11][12] and also fix some notations. The relevant geometry is simple and possesses lots of isometries, yet there are many difficulties in its fundamental level. We also notice [13], which considered some universal time dependent deformations in the context of Schrödinger geometry. One of the deformations is essentially the same as that of [12], yet the discussion was brief and not developed to the degree done in [12].

Then we develop the basic two-point correlation functions from a background called AdS in light-cone [5, 6, 15, 26] following [11][12]. On the way, we develop several conceptually important points of the applications of AdS/CFT on time dependent backgrounds. They include

- i) Establishing the holographic aging equation which describes non-equilibrium critical phenomena,
- ii) Non-trivial radial fall offs of wave function, which are different from the conformal dimensions of the corresponding field, and
- iii) Utilizing the x^- coordinate as an internal direction from the point of view of holography, which gives an alternative way to get real two-time correlators instead of complexifying the geometry done in [12].

To make a clear distinction between these two approaches, we refer Aging background and Schrödinger background for the geometric realization with the additional terms in the background [3][4][12], while we use the term Aging in light-cone and AdS in light-cone for [5][6][26].

2.1 Zero Temperature Aging Background : A Review

Starting with the Schrödinger background [3][4]

$$ds^2 = r^2 \left(d\vec{y}^2 - 2dx^+ dx^- - \tilde{\beta}^2 r^2 dx^{+2} \right) + \frac{dr^2}{r^2} , \quad (1)$$

the following Aging background is constructed in [12]

$$ds^2 = r^2 \left[d\vec{y}^2 - 2dx^+ dx^- - \left(\tilde{\beta}^2 r^2 + \frac{\tilde{\alpha}\tilde{\beta}}{x^+} \right) dx^{+2} \right] - 2\tilde{\alpha}\tilde{\beta} r dr dx^+ + \frac{dr^2}{r^2} . \quad (2)$$

This turns out to be one of the simplest time dependent background which possesses a large number of isometries called aging symmetry with dynamical exponent $z=2$. The Dilatation scaling symmetry D is associated with the transformations, $\vec{y} \rightarrow \lambda \vec{y}$, $x^+ \rightarrow \lambda^2 x^+$ and $x^- \rightarrow x^-$. Other relevant symmetries are spatial translations P_i , Galilean boosts K_i , rotations R_{ij} , central element M interpreted as a particle number and the special conformal transformation C , while the time translational symmetry is broken by the explicit time dependence of the metric *globally*. We come back to this below.

There exist several valuable observations in [12], which are related to the geometry in equation (2) and worthwhile to be mentioned:

- The metric (2) is connected to the Schrödinger background (1) by a local, but *singular*, coordinate transformation

$$x^- \longrightarrow x^- - \frac{\tilde{\alpha}\tilde{\beta}}{2} \ln(r^2 x^+) . \quad (3)$$

This singular time dependent coordinate change is a key to realize aging symmetry. It does not generate curvature singularities at any point in spacetime. It is argued in [12] that this coordinate singularity in this context is similar to a black hole horizon, where physical boundary conditions are imposed, and thus has profound effects, from the gauge/gravity point of view. This geometry is called *locally Schrödinger* in [12]. Thus it is important to impose physical boundary conditions on the time boundaries in addition to the spatial boundaries.

- Thus, locally, the Aging background has the full Schrödinger symmetry with modified set of generators, especially the time translation (H_A) and special conformal transformation (C_A) generators as

$$\begin{aligned} H_A &= \partial_{x^+} - \frac{\tilde{\alpha}\tilde{\beta}}{2x^+} \partial_{x^-} , \\ C_A &= -x^+ r \partial_r + x^+ \vec{y} \cdot \vec{\partial} + x^{+2} \partial_{x^+} + \frac{1}{2} \left(\vec{y}^2 + \frac{1}{r^2} - \tilde{\alpha}\tilde{\beta} x^+ \right) \partial_{x^-} . \end{aligned} \quad (4)$$

The other relevant symmetry generators are not changed by the coordinate transformation (3) [12]. Globally the time translation symmetry is broken and the aging symmetry is realized as conformal Schrödinger symmetry modulo time translation, and described by the generators $\{R_{ij}, P_i, K_i, D, C, M\}$.

- The analysis is done with the complex x^+ , especially at $x^+ = 0$, and also the geometry is extended to be complex with complexified parameter $\tilde{\alpha}$ in [12]. With real $\tilde{\alpha}$, the resulting correlator has the time dependence only in its phase. To achieve a relaxation process, $\tilde{\alpha}$ should be complex.

We show that there is a way out from complexifying the geometry by utilizing the fact that x^- can be considered as an *internal* coordinate from the holographic point of view.

2.2 Aging in Light-Cone

In a similar manner, we start with the AdS in light-cone [5, 6]

$$ds^2 = r^2 (d\bar{y}^2 - 2dx^+ dx^-) + \frac{dr^2}{r^2} , \quad (5)$$

which is shown to be another viable candidate for the Schrödinger holography. This metric can be obtained from the AdS metric with the following coordinate change

$$x^+ = b(t + x) , \quad x^- = \frac{1}{2b}(t - x) . \quad (6)$$

This coordinate transformation was introduced in [15][26][27] and should be viewed as a two-step procedure: a boost in the x -direction with rapidity $\log b$, followed by transforming to light-cone coordinates. To ensure $z=2$, we assign $[b]$ (the scaling dimension of b in the unit of mass) as -1 , and thus $[y_i] = -1$, $[x^+] = -2$ and $[x^-] = 0$. To achieve the desired Schrödinger isometry, it is further required to identify the coordinate x^+ as time and also to have a momentum projection along the other coordinate x^- . x^- direction provides an isometry to the background and thus the corresponding momentum gives the central element M which serves as the total particle number or the mass of the resultant non-relativistic theory. Furthermore this AdS in light-cone is known to have a well defined holographic renormalization and as simple as the case of AdS black holes [26].³

It has been known that the Schrödinger background and the AdS in light-cone share the same physical properties such as thermodynamic [15, 26] and transport properties [26]. We

³See *e.g.* [30][31] for holographic renormalization in general, [32] for Schrödinger background using modified definition of the stress tensor, and [33] for general anisotropic backgrounds using anisotropic scaling.

would like to investigate whether this similarity extends to this time dependent settings or not.

With the *singular* coordinate transformation (3) and a notation change $\tilde{\alpha}\tilde{\beta} \rightarrow \alpha$, we obtain the following metric

$$ds^2 = r^2 \left(d\bar{y}^2 - 2dx^+ dx^- - \frac{\alpha}{x^+} dx^{+2} \right) - 2\alpha r dr dx^+ + \frac{dr^2}{r^2}, \quad (7)$$

which is simpler than that of the Aging background (2). One may note that α is a dimensionless parameter. It can be shown that this metric shares the similar properties as the geometry (2), mentioned in the previous section 2.1. First, the metric (7) is locally AdS in light-cone, while time translation symmetry is broken globally by the *singular* coordinate transformation which connects these two metrics (7) and (5). Second, the isometry of the metric (7) is aging symmetry with the same set of the generators given in (4).

With these properties in mind, let us investigate the background (7). For this purpose, we change the coordinate as $u = \frac{L^2}{r}$ and concentrate on the five dimensional background with $d\bar{y}^2 = dy_1^2 + dy_2^2$ and the metric becomes

$$ds_u^2 = \frac{L^2}{u^2} \left(dy_1^2 + dy_2^2 - 2dx^+ dx^- - \frac{\alpha}{x^+} dx^{+2} + \frac{2\alpha}{u} du dx^+ + du^2 \right), \quad (8)$$

where the boundary sits at $u = 0$. Let us couple the background with a probe scalar ϕ , whose action has the following form

$$S = K \int d^4x \int_{u_B}^{\infty} du \sqrt{-g} \left(g^{uu} \partial_u \bar{\phi} \partial_u \phi + g^{ux^-} \partial_u \bar{\phi} \partial_{x^-} \phi + g^{ux^-} \partial_{x^-} \bar{\phi} \partial_u \phi + g^{\mu\nu} \partial_\mu \bar{\phi} \partial_\nu \phi + m^2 \bar{\phi} \phi \right), \quad (9)$$

where $K = -\pi^3 L^5 / 4\kappa_{10}^2$ and $\mu, \nu = +, -, y, z$. We used u_B for the boundary cutoff, which is small and will be sent to zero eventually. The linearized field equation for ϕ becomes

$$\begin{aligned} 2M \left(i \frac{\partial}{\partial x^+} + \frac{\alpha M}{2x^+} \right) \phi \\ = \frac{\partial^2 \phi}{\partial u^2} + (2iM\alpha - 3) \frac{1}{u} \frac{\partial \phi}{\partial u} - \left(\frac{4iM\alpha + \alpha^2 M^2 + m^2 L^2}{u^2} + \vec{\nabla}^2 \right) \phi. \end{aligned} \quad (10)$$

Note that here we treat x^- coordinate special and replace all the ∂_{x^-} as iM , because this coordinate plays a distinguished role in the Schödinger holography. Later on we consider the parameter M to be either *real* or *imaginary*, from the observation that the coordinate x^- can be treated as an internal coordinate from the field theory point of view.

2.3 Two-point Correlation Function

To find the solution of the equation (10), we use the Fourier decomposition as

$$\phi(u, x^+, \vec{y}) = \int \frac{d\omega}{2\pi} \frac{d^2k}{(2\pi)^2} e^{i\vec{k}\cdot\vec{y}} T_\omega(x^+) f_{\omega, \vec{k}}(u) \phi_0(\omega, \vec{k}) , \quad (11)$$

where \vec{k} is the momentum vector for the corresponding coordinates \vec{y} . $\phi_0(\omega, \vec{k})$ is introduced for the calculation of the correlation functions and is determined by the boundary condition with the normalization $f_{\omega, \vec{k}}(u_B) = 1$. And $T_\omega(x^+)$ is the kernel of integral transformation that convert ω to x^+ , which is necessary for our time dependent setup.

With this Fourier mode, the differential equation (10) decomposes into time dependent part and radial coordinate dependent part. The time dependent equation and its solution read

$$\left(\frac{\alpha M}{2x^+} + i\partial_+ \right) T_\omega = \omega T_\omega \quad \longrightarrow \quad T_\omega(x^+) = c_1 \exp^{-i\omega x^+} (x^+)^{\frac{i\alpha M}{2}} . \quad (12)$$

The radial dependent equation is given by

$$u^2 f''_{\omega, \vec{k}} + (2iM\alpha - 3)u f'_{\omega, \vec{k}} - \left(4iM\alpha + \alpha^2 M^2 + m^2 L^2 + u^2 \vec{k}^2 \right) f_{\omega, \vec{k}} = 2M\omega u^2 f_{\omega, \vec{k}} , \quad (13)$$

where $f' = \partial_u f$. An analytic solution is available in terms of Bessel functions as

$$f_{\omega, \vec{k}} = u^{2-i\alpha M} (c_2 I_\nu(qu) + c_3 K_\nu(qu)) , \quad (14)$$

where I_ν and K_ν are Bessel functions with $\nu = \sqrt{4 + L^2 m^2}$ and $q = \sqrt{\vec{k}^2 + 2M\omega}$.

For this solution to be well defined, we need to impose two different physical boundary conditions, one in deep inside the bulk and another at $x^+ = 0$, because we consider only $x^+ \geq 0$. To have a well defined field deep in the bulk, we choose K over I ,

$$f_{\omega, \vec{k}} = c u^{2-i\alpha M} K_\nu(qu) , \quad (15)$$

which is exponentially converging for large u , deep in the bulk. Thus the full solution is

$$\phi(u, x^+, \vec{y}) = \int \frac{d^2k}{(2\pi)^2} \frac{d\omega}{2\pi} e^{i\vec{k}\cdot\vec{y} - i\omega x^+} u^2 \left(\frac{\alpha x^+}{u^2} \right)^{\frac{i\alpha M}{2}} c K_\nu(qu) \phi_0(\omega, \vec{k}) . \quad (16)$$

Thus we confirm that the aging scalar function is scale-invariant prefactor $\left(\frac{\alpha x^+}{u^2} \right)^{\frac{i\alpha M}{2}}$ times that of the Schrödinger background, advertised in [12]

$$\phi_{\text{Aging}}(u, x^+, \vec{y}) = \left(\frac{\alpha x^+}{u^2} \right)^{\frac{i\alpha M}{2}} \phi_{\text{Schrödinger}}(u, x^+, \vec{y}) . \quad (17)$$

We consider the x^- coordinate as the one for the internal manifold and restrict the system to be a sector with an eigenvalue M . The parameter M would be real if the x^- coordinate is periodic as in discrete light cone quantization. We assume that the x^- has boundaries, for example, at $x^- = 0$ and take M to be a general complex number. This seems to accord with the the boundary at $x^+ = 0$. It would be natural to expect that the imaginary M would represent the dissipative behavior of the system. Let us consider the radial fall offs of the wave solution of the scalar field with the conformal dimension $2 - \nu$. At the boundary $u \rightarrow 0$, the solution behaves as

$$f_{\omega, \vec{k}} \sim u^{2-\nu} u^{-i\alpha M} \sim u^{2-\nu+\alpha M_I} u^{-i\alpha M_R}, \quad \text{with } M = M_R + iM_I. \quad (18)$$

Note that we consider complex $M = M_R + iM_I$ for notational simplicity. Below, we will consider real $M = M_R$ and imaginary $M = iM_I$ cases separately to make the distinction clear.

It is worthwhile to pause and have some comments. First, the conformal dimension of the scalar field ϕ is the same as in AdS in light-cone because the factor $\left(\frac{\alpha x^+}{u^2}\right)^{\frac{i\alpha M}{2}}$ is scale invariant and thus does not contribute to the scaling dimension, which is observed in [12]. Second, as a result, the fall-off behavior of the scalar wave solution at the boundary changes for the case $M = iM_I$. This explicitly demonstrates that the correct scaling dimension of some operators can not be read off just from the behavior of the radial wave solution in the time dependent holography. Third, this change of the radial wave solution can be viewed as "wave function renormalization" and should not be canceled by additional counter terms, as observed in [12]. Physical quantities would have appropriate time dependence to compensate this extra effect. This will be explicitly demonstrated by evaluating the correlation functions below.

We further require the scalar wave solution to behave well as it approaches to $x^+ \rightarrow 0$, because $x^+ = 0$ also serves as a boundary. This is similar to the boundary condition imposed deep inside the bulk along the u -direction, which leads physically reasonable results below. To check the behaviors, we calculate the wave solution, equation (16), near the boundary in coordinate space for the massless case $m = 0$ with $M = iM_I$, $\nu = 2$ and $\phi_0(\omega, \vec{k}) = 1$ as

$$\theta(x^+)(x^+)^{-\frac{\alpha M_I}{2}-1} \exp\left\{-\frac{M_I \vec{y}^2}{2x^+}\right\}. \quad (19)$$

This shows the typical behaviors of the wave solution in the coordinate space. One sees that the wave solution converges at $x^+ = 0$ for $M_I > 0$ due to the exponential factor and also converges at $x^+ \rightarrow \infty$ for $\frac{\alpha M_I}{2} + 1 > 0$ due to the polynomial factor. This demonstrates the convergence of the wave solution at the time boundaries for the imaginary $M = iM_I$. From the fact that the asymptotic forms of the wave solution and two point correlation function

are restricted by aging symmetry, one expects to get similar exponential and polynomial factors for more general cases.

We follow [34][35][36][37] to compute the correlation functions by introducing a cutoff u_B near the boundary and normalizing $f_{\omega, \vec{k}}(u_B) = 1$, which fixes $c = u_B^{-2+i\alpha M} K_\nu^{-1}(qu_B)$. Let us consider the on-shell action, which has two different contributions, the terms proportional to g^{uu} and to g^{u-} , as

$$S[\phi_0] = \int d^3x \frac{L^5}{u^5} \phi^*(u, x^+, \vec{y}) \left(\frac{u^2}{L^2} \partial_u + iM \frac{\alpha u}{L^2} \right) \phi(u, x^+, \vec{y})|_{u_B}. \quad (20)$$

This can be recast using the equation (16) as

$$\begin{aligned} & \int dx^+ \theta(x^+) \frac{d\omega'}{2\pi} \frac{d\omega}{2\pi} e^{-i(\omega' - \omega)x^+} (\alpha x^+)^{-\frac{i\alpha(M^* - M)}{2}} \\ & \times \int d^2y \int \frac{d^2k'}{(2\pi)^2} \int \frac{d^2k}{(2\pi)^2} e^{i(\vec{k}' - \vec{k}) \cdot \vec{y}} \phi_0^*(\omega', \vec{k}') \mathcal{F}(u, \omega', \omega, \vec{k}', \vec{k}) \phi_0(\omega, \vec{k})|_{u_B}, \end{aligned} \quad (21)$$

where $\theta(x^+)$ represents the existence of the physical boundary along the time direction as $0 \leq x^+ < \infty$, and \mathcal{F} is given by

$$\mathcal{F}(u, \omega', \omega, \vec{k}', \vec{k}) = \frac{L^5}{u^5} f_{\omega', \vec{k}'}^*(\omega', \vec{k}', u) \left(\frac{u^2}{L^2} \partial_u + iM \frac{\alpha u}{L^2} \right) f_{\omega, \vec{k}}(\omega, \vec{k}, u). \quad (22)$$

Note that the spatial integration along \vec{y} can be done to give delta function $\delta^2(\vec{k}' - \vec{k})$. One can bring the $u^{\pm i\alpha M}$ factors in f and f^* together to cancel each other, which removes the second part in \mathcal{F} . Then using the relation

$$\frac{\partial}{\partial u} u^2 K_\nu(qu) = u \{ (2 - \nu) K_\nu(qu) - qu K_{\nu-1}(qu) \}, \quad (23)$$

one can evaluate the u -dependent part at $u = u_B$ at the boundary by expanding in terms of small u_B to obtain the non-trivial contribution in \mathcal{F} as

$$\mathcal{F}(u_B, \omega, \vec{k}) = -\frac{2\Gamma(1 - \nu)}{\Gamma(\nu)} \left(\frac{L^3}{u_B^4} \right) \left(\frac{qu_B}{2} \right)^{2\nu} + \dots. \quad (24)$$

Note that the function \mathcal{F} is only function of ω and \vec{k} when it is evaluated at the boundary. Thus the time independent part is the same as previously considered cases in [4] [5][12]. But this is not the end of the story. To obtain the final form of the momentum correlation function, we need to evaluate the time dependent part. Here we consider two cases, $M = M_R$ and $M = iM_I$ with real parameters M_R and M_I , separately.

2.3.1 $M = M_R$

One can perform the x^+ integration in equation (21) to get the following results, because of the step function and vanishing exponent, $M^* - M = 0$,

$$\mathcal{G}(\omega' - \omega) = \frac{\delta(\omega' - \omega)}{2} - \frac{i}{2\pi(\omega' - \omega)} . \quad (25)$$

Thus the momentum correlation function has two parts

$$\langle \mathcal{O}^*(\omega', \vec{k}') \mathcal{O}(\omega, \vec{k}) \rangle = -2(2\pi)^{-3} \delta(\vec{k}' - \vec{k}) \mathcal{F}(u_B, \omega, \vec{k}) \mathcal{G}(\omega' - \omega) , \quad (26)$$

where \mathcal{F} is given in equation (24). This is the final form of the momentum space correlation functions. Note the extra term present due to our boundary condition with step function in time domain.

Let us evaluate the coordinate correlation function as⁴

$$\begin{aligned} & \langle \mathcal{O}^*(x_2^+, \vec{y}_2) \mathcal{O}(x_1^+, \vec{y}_1) \rangle \\ &= \int \frac{d\omega'}{2\pi} \frac{d^2 k'}{(2\pi)^2} \frac{d\omega}{2\pi} \frac{d^2 k}{(2\pi)^2} e^{i\vec{k}' \cdot \vec{y}_2 - i\vec{k} \cdot \vec{y}_1} e^{-i\omega' \cdot x_2^+ + i\omega \cdot x_1^+} \left(\frac{x_2^+}{x_1^+} \right)^{i\frac{\alpha M_R}{2}} \langle \mathcal{O}^*(\omega', \vec{k}') \mathcal{O}(\omega, \vec{k}) \rangle . \end{aligned} \quad (28)$$

For further calculations, we use the following integral

$$\int \frac{d\omega'}{2\pi} e^{-i(\omega' - \omega)x_2^+} \mathcal{G}(\omega' - \omega) = \frac{1 + \text{sign}(x_2^+)}{2} = \theta(x_2^+) , \quad (29)$$

with the condition $x_2^+ > 0$, and the inverse transform of $q^{2\nu}$ as

$$\frac{M_R^{1+\nu}}{\pi 2^{1-\nu} i^{1+\nu} \Gamma(-\nu)} \frac{\theta(x_2^+ - x_1^+)}{(x_2^+ - x_1^+)^{2+\nu}} \exp \left(i M_R \frac{(\vec{y}_2 - \vec{y}_1)^2}{2(x_2^+ - x_1^+)} \right) , \quad (30)$$

⁴Note the time dependent factor $(x^+)^{-i\frac{\alpha M_R}{2}}$ in front of the boundary scalar operator is opposite to that of the corresponding scalar field in (16). The scaling dimension of the aging scalar operator is effectively different by $i\alpha M$ compared to that of the Schrödinger case

$$[\phi_{\text{aging}}] = [\phi_{\text{Schrödinger}}] + i\alpha M , \quad (27)$$

as read off from the radial fall-offs in equation (17). This should be compensated by an appropriate time dependent factor. Another way to see this is the relation

$$\langle \mathcal{O}(1) \dots \rangle = \frac{\delta}{\delta \phi_0(1)} \dots e^{\int_{\partial} \mathcal{O} \phi_0} ,$$

where the time dependent factor would result in opposite way. This is the same for the case with $M = iM_I$ discussed below.

where we used $(\vec{y}_2 - \vec{y}_1)^2 > 0$ and $x_2^+ - x_1^+ > 0$. Then the coordinate space correlation function is

$$\begin{aligned}
& -2 \left(\frac{x_2^+}{x_1^+} \right)^{i\frac{\alpha M_R}{2}} \int \frac{d\omega}{2\pi} \frac{d^2 k}{(2\pi)^2} e^{-i\vec{k} \cdot (\vec{y}_1 - \vec{y}_2)} e^{i\omega(x_1^+ - x_2^+)} \cdot \int \frac{d\omega'}{2\pi} e^{-i(\omega' - \omega)x_2^+} \mathcal{G}(\omega' - \omega) \cdot \mathcal{F}(u_B, \omega, \vec{k}) \\
& = \frac{\Gamma(1 - \nu)}{\Gamma(\nu)\Gamma(-\nu)} \frac{L^3 M_R^{1+\nu}}{\pi 2^{\nu-1} i^{1+\nu} u_B^{4-2\nu}} \cdot \frac{\theta(x_2^+) \theta(x_2^+ - x_1^+)}{(x_2^+ - x_1^+)^{2+\nu}} \left(\frac{x_2^+}{x_1^+} \right)^{i\frac{\alpha M_R}{2}} \exp \left(i \frac{M_R (\vec{y}_2 - \vec{y}_1)^2}{2(x_2^+ - x_1^+)} \right) . \quad (31)
\end{aligned}$$

This is our main result for the zero temperature correlation function with $M = M_R$. We would like to pause to comment:

- We find that the time dependent polynomial part is the same as the result [12] when $M = M_R$. This is associated with the fact the the scaling dimension of a boundary scalar operator is opposite to that of the source of the corresponding scalar field.

$$\langle \mathcal{O}^*(x_2^+, \vec{y}_2) \mathcal{O}(x_1^+, \vec{y}_1) \rangle_{\text{Aging}} = \left(\frac{x_1^+}{x_2^+} \right)^{-\frac{i\alpha M_R}{2}} \langle \mathcal{O}^*(x_2^+, \vec{y}_2) \mathcal{O}(x_1^+, \vec{y}_1) \rangle_{\text{Schrödinger}} . \quad (32)$$

- It turns out that there exist only oscillating behaviors for $M = M_R$. Thus the same is true for real value for αM , because there exists only the combination αM .
- For the massless case with $\nu = 2$, we have

$$\mathcal{F}(u_B, \omega, \vec{k}) = -\frac{L^3}{8} q^4 \log(q^2) + \dots . \quad (33)$$

Thus the coordinate space correlation function is given by

$$\begin{aligned}
& \langle \mathcal{O}^*(x_2^+, \vec{y}_2) \mathcal{O}(x_1^+, \vec{y}_1) \rangle \\
& = -\frac{iL^3 M_R^3}{\pi} \cdot \frac{\theta(x_2^+) \theta(x_2^+ - x_1^+)}{(x_2^+ - x_1^+)^{2+\nu}} \left(\frac{x_2^+}{x_1^+} \right)^{i\frac{\alpha M_R}{2}} \exp \left(i \frac{M_R (\vec{y}_2 - \vec{y}_1)^2}{2(x_2^+ - x_1^+)} \right) . \quad (34)
\end{aligned}$$

2.3.2 $M = iM_I$

Let us evaluate the time integral first. We perform the Fourier transform for the time range $0 \leq x^+ < \infty$, and define $\mathcal{G}(w) = \int dx^+ e^{iwx^+} \theta(x^+) \cdot (\alpha x^+)^{-\alpha M_I}$. Then

$$\mathcal{G}(w) = \alpha^{-\alpha M_I} |w|^{-1+\alpha M_I} \Gamma(1 - \alpha M_I) \left(-i \cos\left(\frac{\pi \alpha M_I}{2}\right) \text{sign}(w) + \sin\left(\frac{\pi \alpha M_I}{2}\right) \right) . \quad (35)$$

where $w = \omega' - \omega$. Note that these results are essentially the same as those evaluated by Laplace transform in, so called, s -domain.

Thus we get the momentum correlation function as

$$\langle \mathcal{O}^*(\omega', \vec{k}') \mathcal{O}(\omega, \vec{k}) \rangle = -2(2\pi)^{-3} \delta(\vec{k}' - \vec{k}) \mathcal{G}(\omega' - \omega) \mathcal{F}(u_B, \omega, \vec{k}) . \quad (36)$$

Again, \mathcal{F} is given in equation (24), and $q = \sqrt{\vec{k}^2 + 2M\omega}$. Here we can have $\vec{k} = 0$ due to the spatial translational invariance, but not for ω because time translation symmetry is broken.

Let us calculate the coordinate space correlation function as

$$\begin{aligned} & \langle \mathcal{O}^*(x_2^+, \vec{y}_2) \mathcal{O}(x_1^+, \vec{y}_1) \rangle \\ &= \int \frac{d\omega'}{2\pi} \frac{d^2 k'}{(2\pi)^2} \frac{d\omega}{2\pi} \frac{d^2 k}{(2\pi)^2} e^{i\vec{k}' \cdot \vec{y}_2 - i\vec{k} \cdot \vec{y}_1} e^{-i\omega' \cdot x_2^+ + i\omega \cdot x_1^+} (\alpha^2 x_1^+ x_2^+)^{\frac{\alpha M_I}{2}} \langle \mathcal{O}^*(\omega', \vec{k}') \mathcal{O}(\omega, \vec{k}) \rangle . \end{aligned} \quad (37)$$

After carrying out the integral for the ω' first

$$\int \frac{d\omega'}{2\pi} e^{i(\omega' - \omega)x_2^+} \mathcal{G}(\omega' - \omega) = \theta(x_2^+) \alpha^{-\alpha M_I} |x_2^+|^{-\alpha M_I} , \quad (38)$$

the expression reduces to the previous case for the time independent part, whose calculation is done similarly. We get

$$\begin{aligned} & \langle \mathcal{O}^*(x_2^+, \vec{y}_2) \mathcal{O}(x_1^+, \vec{y}_1) \rangle \\ &= -2\theta(x_2^+) (\alpha^2 x_1^+ x_2^+)^{\frac{\alpha M_I}{2}} \alpha^{-\alpha M_I} |x_2^+|^{-\alpha M_I} \int \frac{d\omega}{2\pi} \frac{d^2 k}{(2\pi)^2} e^{-i\vec{k} \cdot (\vec{y}_1 - \vec{y}_2)} e^{i\omega(x_1^+ - x_2^+)} \mathcal{F}(u_B, \omega, \vec{k}) \\ &= \frac{\Gamma(1 - \nu)}{\Gamma(\nu)\Gamma(-\nu)} \frac{L^3 M_I^{1+\nu}}{\pi 2^{\nu-1} u_B^{4-2\nu}} \cdot \frac{\theta(x_2^+) \theta(x_2^+ - x_1^+)}{(x_2^+ - x_1^+)^{2+\nu}} \cdot \left(\frac{x_2^+}{x_1^+} \right)^{-\frac{\alpha M_I}{2}} \cdot \exp \left(-\frac{M_I (\vec{y}_2 - \vec{y}_1)^2}{2(x_2^+ - x_1^+)} \right) . \end{aligned} \quad (39)$$

This is the result we are looking for. This confirms that the correlation function has dissipative behavior for $M = iM_I$. Thus

- We find that the time dependent polynomial part is identical to the result [12] when $M = M_R$. This is associated with the fact the the scaling dimension of a boundary scalar operator is opposite to that of the source of the corresponding scalar field.

$$\langle \mathcal{O}^*(x_2^+, \vec{y}_2) \mathcal{O}(x_1^+, \vec{y}_1) \rangle_{\text{Aging}} = \left(\frac{x_2^+}{x_1^+} \right)^{-\frac{\alpha M_I}{2}} \langle \mathcal{O}^*(x_2^+, \vec{y}_2) \mathcal{O}(x_1^+, \vec{y}_1) \rangle_{\text{Schrödinger}} . \quad (40)$$

- There exist only the combination αM , and thus the result is true for imaginary αM .
- For the massless case with $\nu = 2$, we have the coordinate space correlation function similar to the $M = M_R$ case as

$$\langle \mathcal{O}^*(x_2^+, \vec{y}_2) \mathcal{O}(x_1^+, \vec{y}_1) \rangle = -\frac{iL^3 M_I^3}{\pi} \cdot \frac{\theta(x_2^+) \theta(x_2^+ - x_1^+)}{(x_2^+ - x_1^+)^{2+\nu}} \left(\frac{x_2^+}{x_1^+} \right)^{-\frac{\alpha M_I}{2}} \exp \left(-\frac{M_I (\vec{y}_2 - \vec{y}_1)^2}{2(x_2^+ - x_1^+)} \right) . \quad (41)$$

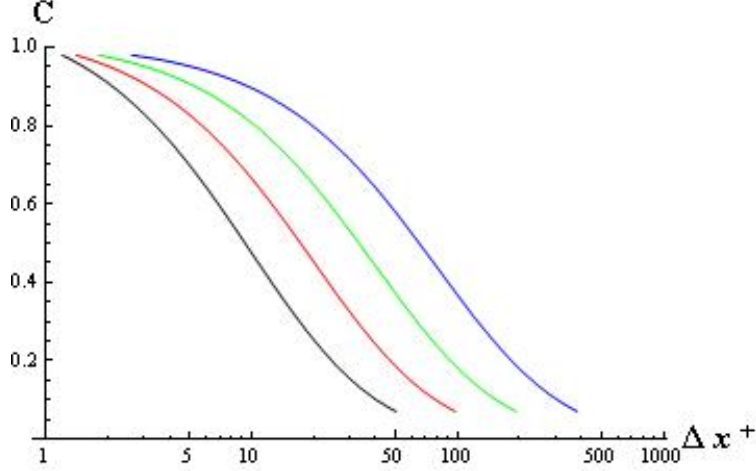


Figure 1: Plot of the equation (42) with $\nu = 0$, $\alpha M_I = 1$, $\alpha M_R = 0$. The horizontal and vertical axes are $\Delta x^+ = x_2^+ - x_1^+$ and two-time correlation function $C = C(x_2^+, x_1^+)$, respectively. The four plots, black, red, green and blue (from left to right) are for the particular waiting time $x_1^+ = 25, 50, 100$, and 200 , respectively. They show that the older is the system the slower it relaxes. This plot is to be compared with that of the numerical results in [10].

2.4 Two-time Correlators

One of the important physical observables considered in the literature (see *e.g.* [9][38]) is two-time correlation functions at the same space positions, which we refer to $C(x_2^+, x_1^+)$

$$C(x_2^+, x_1^+) = \langle \mathcal{O}^*(x_2^+, \vec{y}_2) \mathcal{O}(x_1^+, \vec{y}_1) \rangle_{\vec{y}_1 = \vec{y}_2} \equiv (x_1^+)^{-\lambda_b} f_C \left(\frac{x_2^+}{x_1^+} \right), \quad (42)$$

where $f_C(x) = x^{-\lambda_C/z}$, and z is the dynamical exponent. x_1^+ and x_2^+ are called a waiting time and a response time, respectively. This scaling behavior is expected to apply for the "aging regime": $x_1^+, x_2^+ \gg x_{mi}^+$ and $x_2^+ - x_1^+ \gg x_{mi}^+$, where x_{mi}^+ is a microscopic time scale of a given system.

Our dual field theory possesses aging invariance, inherited from the bulk gravity and hence exhibits two important characteristic features of aging system, namely the time dependence and the existence of dynamical scaling. Furthermore, for $M_R = 0$ and for $x_2^+ \gg x_1^+$, which is physically interesting aging regime, our two-time correlation function decays slowly following power law, like (42), with

$$\lambda_b = \nu + 2, \quad \lambda_C = z \left(\nu + 2 + \frac{\alpha M_I}{2} \right), \quad (43)$$

where $z = 2$ for our case. These two parameters λ_b and λ_C are our physical exponents associated with the two-time correlation function. The dissipating behaviors of the correlation function are plotted in figure 1 with several different waiting time. We clearly see the typical aging behavior: older systems relax in a slower manner than younger systems, and thus the correlation between two different time x_1^+ and x_2^+ has more correlation for the bigger waiting time x_1^+ in our correlation function $C(x_2^+, x_1^+)$.

2.5 Comments on Schrödinger Background

In this section, we would like to briefly comment on the aging construction on the Schrödinger background [12] with our approach, especially with the complex M and without complexifying the spacetime geometry.

Schrödinger background can be embedded in string theory in a nice way using null Melvin twist [19][20]. Previous sections already confirmed that the results of the scalar wave solution and the two-point correlation function are the same for both cases even though these two approaches are rather different. This is mainly because the Schrödinger symmetry is large enough to restrict the physical properties of two point correlation functions. It is still worthwhile to revisit the aging construction for the Schrödinger background with our approach.

Let us consider the following metric with the change $x^+ \rightarrow t$, $u \rightarrow z$ and $x^- \rightarrow \xi$

$$ds^2 = \frac{L^2}{z^2} \left(dz^2 - \frac{1}{z^2} dt^2 - 2dt d\xi + d\bar{y}^2 \right) + \frac{L^2}{z^2} \left(\frac{2\alpha}{z} dz dt - \frac{\alpha}{t} dt^2 \right), \quad (44)$$

where extra matter contents, which are not explicitly written here, are necessary to support this background. Following the previous section, we couple a scalar field to this background. We find the identical radial differential equation as the one in AdS in light-cone if we change, $m^2 \rightarrow m'^2 = m^2 + M^2/L^2$ [5].

For the complex parameter $M = M_R + iM_I$, the form of the corresponding solution is the same as (16) with $q = \sqrt{\vec{k}^2 + 2M\omega}$ and $\nu' = \sqrt{4 + L^2 m^2 + M^2}$. These parameters were used in the Schrödinger background [3][4]. Again we confirm that the aging scalar wave solution is given by the scale-invariant factor, $(\alpha x^+/u^2)^{\frac{i\alpha M}{2}}$, times the Schrödinger wave solution as advertised in [12]. This is given in (17). With this in hand, it is straightforward to evaluate the two-point correlation function, which is also the same as that of the AdS in light-cone and is given in equations (31) for $M = M_R$ and (39) for $M = iM_I$. Thus, at zero temperature, the physical properties of Aging in light-cone are the same as those of the Aging background for the operators with the same scaling dimensions, $\nu = \nu'$. The scaling dimension of the operator ϕ is complex in general for complex M . If we consider either real $M = M_R$ or pure

imaginary $M = iM_I$, which are physically interesting cases, the scaling dimension is still real. It is interesting to notice that the scaling dimension $\Delta_\phi = 2 - \nu'$ decreases for the real $M = M_R$, while it increases for imaginary $M = iM_I$.

All the other discussions and physical properties remain unchanged compared to the Aging in light-cone at zero temperature. Interestingly enough, as we will see later, these do not persist at the finite temperature.

2.6 Comments on Dual Field Theory

In the context of the holographic condensed matter application, the field theory dual of the gravity description is not explicitly known in most cases. For the case of the Schrödinger geometry, the situation is much better because the construction are explicitly known as Discrete Light-Cone Quantization (DLCQ) for AdS in light-cone and null Melvin twist for the Schrödinger background. The basic field theory dual of AdS in light-cone is DLCQ of the $\mathcal{N} = 4$ Super Yang-Mills theory proposed in [39][40] as explained in [15]. It is further required to project the conserved particle number M to a single sector, which is related to the isometry of the gravity backgrounds and has distinguished role [3, 5, 6, 26]. We are required to focus on a single sector of the particle number. For further developments along the Schrödinger background with null Melvin twist, see [16]. In this section we would like to comment on some properties directly related to the time dependent generalizations of the setup, which apply for both AdS in light-cone and Schrödinger backgrounds.

The differential equation (10), we consider at the end of section 2.2, has an explicit time dependence. Thus the dual boundary field theory is expected to have not Schrödinger but aging symmetries. From the observation that the equation (10) factorize into u -dependent and u -independent parts, we factorize $\phi = \varphi(x^+, \vec{y}) f(u)$ and find that the boundary wave function φ satisfies the following differential equation

$$2M \left(i \frac{\partial}{\partial x^+} + \frac{\alpha M}{2x^+} \right) \varphi + \vec{\nabla}^2 \varphi - v^2 \varphi = 0 , \quad (45)$$

where v^2 is the eigenvalue of the radial differential equation. The term $v^2 \varphi$ can be interpreted as the one coming from the variation of the Landau-Ginzburg potential, i.e. $\frac{\delta \mathcal{V}_{LG}}{\delta \varphi} = v^2 \varphi$. One may generate the general Landau-Ginzburg potential by considering the self-interacting scalar fields in bulk. It is clear that our geometric realization of aging symmetry actually constrains the nature of the time dependence of the equation of the dual field theory as the form

$$\frac{\alpha M^2}{x^+} \varphi . \quad (46)$$

It is interesting to note that if we can add noise contributions the differential equation becomes the Langevin equation [41].

It is not difficult to solve the differential equation (45) and read off the time dependent part of the solution. Compared to the $\alpha = 0$ case we get

$$\varphi \longrightarrow (x^+)^{\frac{i\alpha M}{2}} \varphi. \quad (47)$$

Thus with aging symmetry, the boundary scalar field will acquire the explicit time-dependence of this form. Note that we can also infer the same conclusion from the local transformation (3) which contains essential effects to the bulk side of the story. Furthermore, the parameter v contains other effects due to the renormalization of the radial coordinate. It turns out that, for real M , there is no net effects of this radial wave function renormalization on physical observables such as the two-point correlation function as we see in (17) and (31)(39).

3 Finite Temperature Aging Holography

We start with the Einstein-Hilbert action with cosmological constant, which admits the planar black hole solution

$$\begin{aligned} ds^2 &= \left(\frac{r}{L}\right)^2 \left[\frac{1-h}{4b^2} (dx^+)^2 - (1+h) dx^+ dx^- + (1-h)b^2 (dx^-)^2 + d\bar{y}^2 \right] \\ &+ \left(\frac{L}{r}\right)^2 \frac{1}{h} dr^2, \quad h = 1 - \frac{r_H^4}{r^4}. \end{aligned} \quad (48)$$

We would like to exploit the idea that the aging metric is locally Schrödinger, and thus we can get the Aging black hole from the Schrödinger black hole using the coordinate transformation as

$$x^- \rightarrow x^- + \frac{\alpha}{2} \ln(r^2 x^+). \quad (49)$$

The black hole metric in the simplest form can be written as

$$\begin{aligned} ds^2 &= \left(\frac{r}{L}\right)^2 \left\{ -\frac{h}{1-h} b^{-2} dx^{+2} + (1-h)b^2 \left(dx^- + \frac{\alpha}{r} dr - \left(-\frac{\alpha}{2x^+} + \frac{1}{2b^2} \frac{1+h}{1-h} \right) dx^+ \right)^2 + d\bar{y}^2 \right\} \\ &+ \left(\frac{L}{r}\right)^2 h^{-1} dr^2. \end{aligned} \quad (50)$$

We would like to consider this finite temperature metric to construct the correlation functions.

3.1 Equation of Motion

We consider a probe scalar on the Aging black hole background and try to evaluate the two-point correlator similar to the previous section. The equation of motion is given by

$$\frac{1}{\sqrt{-g}}\partial_\mu(\sqrt{-g}g^{\mu\nu}\partial_\nu\phi) - m^2\phi = 0. \quad (51)$$

The metric depends only on (x^+, r) and the equations of motion can be expressed as

$$\frac{r}{L^2}(4+h)\partial_r\phi - \frac{4\alpha}{L^2}\partial_-\phi - \frac{L^2}{r^2}\frac{\alpha b^2}{2(x^+)^2}\frac{1-h}{h}\partial_-\phi + g^{\mu\nu}\partial_\mu\partial_\nu\phi - m^2\phi = 0. \quad (52)$$

As was done in the previous section, we replace the derivative of the x^- coordinate as $\partial_{x^-} = iM$. The mode expansion becomes of the form,

$$\phi(r, x^+, \vec{y}) = \int \frac{d\omega}{2\pi} \frac{d^2k}{(2\pi)^2} \exp^{-i\vec{k}\cdot\vec{y}} \phi_k(r, x^+) \phi_0(\omega, \vec{k}), \quad (53)$$

where $\phi_k(r, x^+) = T_\omega(x^+) f_{\omega, \vec{k}}(r)$.

The equation of motion in r coordinate is complicated. It is slightly better to go to a different coordinate using $z = \frac{r_H^2}{r^2}$. Then the differential equation is

$$\begin{aligned} & \frac{L^4}{4zhr_H^2} \left(\frac{1+h}{h} M \frac{\hat{D}T_\omega}{T_\omega} - \frac{(1-h)b^2}{h} \frac{\hat{D}^2T_\omega}{T_\omega} \right) \\ &= \frac{f''_{\omega, \vec{k}}}{f_{\omega, \vec{k}}} - \frac{(-i\alpha Mh - h + 2)}{zh} \frac{f'_{\omega, \vec{k}}}{f_{\omega, \vec{k}}} - \left(\frac{4i\alpha M + \alpha^2 M^2 h + m^2 L^2}{4z^2 h} + \frac{\vec{k}^2 - \frac{M^2}{4b^2} \frac{1-h}{h}}{4zhr_H^2/L^4} \right), \end{aligned} \quad (54)$$

where $f' = \partial_z f$, and we used

$$\hat{D} \equiv i \frac{\partial}{\partial x^+} + \frac{\alpha M}{2x^+}, \quad h = 1 - z^2. \quad (55)$$

One qualitatively different feature from zero temperature case is that this finite temperature version of the differential equation does have a second order time derivative term. Yet as we see in the first line of equation (54), this does not generate different dynamics along time direction compared to the zero temperature case because the time dependent parts of the differential equation, equation (54) factorize in a special way.

The time dependent part can be solved as follows:

$$\left(\frac{\alpha M}{2x^+} + i\partial_+ \right) T_\omega = \omega T_\omega \quad \longrightarrow \quad T_\omega(x^+) = c_1 \exp^{-i\omega x^+} (x^+)^{\frac{i\alpha M}{2}}. \quad (56)$$

Thus, we would like to stress that, the time dependent part of the scalar wave solution at finite temperature is exactly the same as that of the zero temperature case. Anticipating the

appearance of the scaling invariant combination, x^+/z , we factorize as $f_{\omega, \vec{k}}(z) = z^{-\frac{i\alpha M}{2}} \tilde{g}_{\omega, \vec{k}}(z)$ and obtain the radial equation:

$$\tilde{g}'' - \frac{1+z^2}{z(1-z^2)} \tilde{g}' - \frac{m^2 L^2}{4z^2(1-z^2)} \tilde{g} + \frac{\mathbf{w}^2 z}{(1-z^2)^2} \tilde{g} - \frac{\mathbf{q}^2}{z(1-z^2)} \tilde{g} = 0 ,$$

where $\mathbf{w} = \frac{M/(2b^2) - \omega}{2\pi T} , \quad \mathbf{q}^2 = \frac{2M\omega + \vec{k}^2}{(2\pi bT)^2} ,$ (57)

where used $r_H = \pi L^2 bT$. The equation includes the term which has the Schrödinger invariant combination $2M\omega + \vec{k}^2$, explicitly, and the term which is partially broken due to the other combination $\mathbf{w} \sim M/(2b) - b\omega$ at finite temperature. The term proportional to \mathbf{w} is dominant at the horizon $z = 1$ and important for the calculation of the correlation functions. Interestingly enough, the combination of chemical potential $\frac{1}{2b^2}$ and conserved charge M of x^- direction of the time-independent Schrödinger black hole shows up with the energy of the probe scalar ω . In what follows, we consider the low energy regime in which the magnitude of the combination $\frac{M}{2b^2}$ is bigger than ω , which corresponds to $\mathbf{w} > 0$.

Note that this equation is nothing but the radial equation for the AdS planar black hole in light-cone. Thus we explicitly check that the radial part of the time independent aging wave solution is the same as that of the AdS in light-cone case. This has an important implication that the time independent part of the aging wave solution and correlation functions are those of the AdS in light-cone at least in momentum space with some modification, which can be identified and thus isolated.

The full solution is

$$\phi(z, x^+, \vec{y}) = \int \frac{d^2 k}{(2\pi)^2} \frac{d\omega}{2\pi} e^{i\vec{k} \cdot \vec{y} - i\omega x^+} \left(\frac{\alpha x^+}{z} \right)^{\frac{i\alpha M}{2}} c \tilde{g}_{\omega, \vec{k}}(z) \phi_0(\omega, \vec{k}) , \quad (58)$$

where the solution has the desired scaling form with an appropriate normalization for the correlator calculation. We concentrate on the momentum space correlation functions from now on.

3.2 Finite Temperature Correlation Functions

In this section, we would like to evaluate the scalar correlation function of the Schrödinger geometry via AdS in light-cone with finite parameters M , ω and \vec{k} , which is fairly non-trivial even in this simple setup. First, we consider the time dependence of the coordinate space correlation functions and outline the general properties of the correlation functions at finite temperature. After that we concentrate on the momentum space correlation functions starting with analytic approaches in general. And then we evaluate the correlation functions

analytically for some special cases and obtain the expression for the shear viscosity, which is presented in appendix C. Finally we get the full features with numerical studies. From the numerical study, we observe two distinct peaks in momentum space correlation functions, one broad peak at the $(\omega, k) = (0, 0)$ and another at finite values of ω and k , which are explained in detail at the end of this section.

3.2.1 General Features

In section (3.1), we have some important observations regarding the time dependence of the scalar equation of motion. Combining with the experience from the zero temperature case in section (2.3), we would like to see the general time dependence of the coordinate space correlation functions.

Following the steps done in section (2.3), we rewrite the solution (58) as

$$\phi(z, x^+, \vec{y}) = \int \frac{d^2 k}{(2\pi)^2} \frac{d\omega}{2\pi} e^{i\vec{k} \cdot \vec{y} - i\omega x^+} (\alpha x^+)^{\frac{i\alpha M}{2}} f_{\omega, \vec{k}}(z) \phi_0(\omega, \vec{k}), \quad (59)$$

where $f_{\omega, \vec{k}}(z) = cz^{-\frac{i\alpha M}{2}} \tilde{g}_{\omega, \vec{k}}(z)$. Then the on-shell action has the form

$$S[\phi_0] = \int d^3 x \sqrt{-g} \phi^*(z, x^+, \vec{y}) (g^{zz} \partial_z + iMg^{z-}) \phi(z, x^+, \vec{y})|_{z_B}. \quad (60)$$

This can be recast using the equation (59) as

$$\begin{aligned} & \int dx^+ \theta(x^+) \frac{d\omega'}{2\pi} \frac{d\omega}{2\pi} e^{-i(\omega' - \omega)x^+} (\alpha x^+)^{-\frac{i\alpha(M^* - M)}{2}} \\ & \times \int d^2 y \int \frac{d^2 k'}{(2\pi)^2} \int \frac{d^2 k}{(2\pi)^2} e^{i(\vec{k}' - \vec{k}) \cdot \vec{y}} \phi_0^*(\omega', \vec{k}') \mathcal{F}(u, \omega', \omega, \vec{k}', \vec{k}) \phi_0(\omega, \vec{k})|_{u_B}, \end{aligned} \quad (61)$$

where $\theta(x^+)$ represents the physical region as $0 \leq x^+ < \infty$, and \mathcal{F} is given by

$$\mathcal{F}(z, \omega', \omega, \vec{k}', \vec{k}) = \sqrt{-g} f_{\omega', \vec{k}'}^*(\omega', \vec{k}', z) (g^{zz} \partial_z + iMg^{z-}) f_{\omega, \vec{k}}(\omega, \vec{k}, z). \quad (62)$$

Note that the spatial integration along \vec{y} can be done to give delta function $\delta^2(\vec{k}' - \vec{k})$. One can bring the $z^{\pm i\frac{\alpha M}{2}}$ factors in f and f^* together to cancel each other, which removes the second part in \mathcal{F} . Then time independent radial part \mathcal{F} of momentum correlation function is given by

$$\mathcal{F}(z, \omega', \omega, \vec{k}', \vec{k}) = \frac{b^4 \pi^4 L^5 T^4}{2z^3} \left(\frac{\tilde{g}_{\omega', \vec{k}'}(z)}{\tilde{g}_{\omega', \vec{k}'}(z_B)} \right)^* \frac{4z^2 h}{L^2} \partial_z \left(\frac{\tilde{g}_{\omega, \vec{k}}(z)}{\tilde{g}_{\omega, \vec{k}}(z_B)} \right). \quad (63)$$

It turns out that evaluating this correlation function is highly nontrivial because the differential equation is not analytically tractable for the AdS in light-cone except some special limits, while it is even more complicated for the Schrödinger background.

Before explaining the time dependent part of the correlation function, we would like to comment on our choice of the incoming boundary condition for the equation (57), which is not clear due to the contribution of M in the \mathbf{w} . We choose our incoming boundary condition as

$$e^{-i\omega x^+}(1-z)^{i\mathbf{w}/2} \propto e^{-i\omega(x^++z_*)} \quad (64)$$

where $z_* = \frac{\ln(1-z)}{4\pi T}$. We come back to this radial dependent part of the correlation function with several different approaches below.

As discussed in the section 2, this is not the end of the story. The time dependent parts turn out to be the same as those of the zero temperature case because their time dependences in the wave solution (58) are the same. This is explained below equation (55). Thus the time dependent parts of the correlation function can be explicitly computed and are given by \mathcal{G} in equations (25) and (35). Explicitly, we get

$$\langle \mathcal{O}^*(\omega', \vec{k}') \mathcal{O}(\omega, \vec{k}) \rangle = -2(2\pi)^{-3} \delta(\vec{k}' - \vec{k}) \mathcal{F}(u_B, \omega, \vec{k}) \mathcal{G}(\omega' - \omega) , \quad (65)$$

where \mathcal{F} is given in equations (63). By performing the ω' integration, the coordinate space correlation function is give by

$$\langle \mathcal{O}^*(x_2^+, \vec{y}_2) \mathcal{O}(x_1^+, \vec{y}_1) \rangle = \theta(x_2^+) \left(\frac{x_2^+}{x_1^+} \right)^{-i\frac{\alpha M}{2}} \langle \mathcal{O}^*(x_2^+, \vec{y}_2) \mathcal{O}(x_1^+, \vec{y}_1) \rangle_{\text{Schrödinger}} . \quad (66)$$

Where M can be either $M = M_R$ or $M = iM_I$. The latter case is related to the dissipative case.

It is not straight forward to evaluate the general momentum space correlation functions analytically, not to mention the coordinate space correlation functions. Thus we would like to concentrate on the momentum space correlation function for the rest of the section.

3.2.2 Analytic Approaches

Let us outline the analytic approach we considered and summarize our observations.

The differential equation (57) has 4 regular singular points, which, in general, can not be solved with systematic approach. If we take

$$\tilde{g}(z) = z^{\frac{1+\bar{\gamma}}{2}} (z-1)^{\frac{-1+\bar{\delta}}{2}} (z+1)^{\frac{-1+\bar{\epsilon}}{2}} G(z) . \quad (67)$$

The differential equation (57) can be cast into the Heun's equation

$$G''(z) + \left(\frac{\bar{\gamma}}{z} + \frac{\bar{\delta}}{z-1} + \frac{\bar{\epsilon}}{z+1} \right) G'(z) + \frac{\bar{\alpha}\bar{\beta}z - \bar{q}}{z(z-1)(z+1)} G(z) = 0 , \quad (68)$$

$$\text{where} \quad 4\bar{\alpha}\bar{\beta} = \nu^2 - 2 + 2(\bar{\gamma}\bar{\delta} + \bar{\delta}\bar{\epsilon} + \bar{\epsilon}\bar{\gamma}) , \quad -2\bar{q} = \mathbf{q}^2 + \bar{\gamma}\bar{\delta} + \bar{\gamma}\bar{\epsilon} , \quad (69)$$

with the special values of

$$\bar{\gamma} = 1 \pm \nu, \quad \bar{\delta} = 1 \pm i\mathbf{w}, \quad \bar{\epsilon} = 1 \pm \mathbf{w}. \quad (70)$$

The general solutions of this equation are known as the Heun functions $Hl(-1, \bar{q}; \bar{\alpha}, \bar{\beta}, \bar{\gamma}, \bar{\delta}; z)$. In general, we have 8 different combination of the parameters $\bar{\gamma}, \bar{\delta}, \bar{\epsilon}$, out of which only 4 solutions are physical due to the incoming boundary condition we would like to impose at $z = 1$. That corresponds to the choice $\bar{\delta} = 1 + i\mathbf{w}$ due to our choice of \mathbf{w} parameter given in equation (57). For special values of parameters, the Heun functions might provide analytic solutions.

We observe that our differential equation (57) is similar to the equation (3.4) of [42], even though they have very different setup. We can rewrite the differential equation (57) in a slightly different way to make the comparison straightforward

$$\tilde{g}'' - \frac{1+z^2}{z(1-z^2)}\tilde{g}' - \left(\frac{L^2 m^2}{4z^2(1-z^2)} + \frac{Q^2 - z^2 Y^2}{z(1-z^2)^2} \right) \tilde{g} = 0. \quad (71)$$

where $Y^2 = \frac{\vec{k}^2 + (M/(2b) + b\omega)^2}{4\pi^2 b^2 T^2}$, $Q^2 = \frac{2M\omega + \vec{k}^2}{4\pi^2 b^2 T^2}$. Note that, in general, $Y^2 \geq Q^2$, where the equality holds when $M = 2\omega b^2$. One of the crucial difference between this equation and (3.4) of [42] lies in the last term. In our case, Y^2 has always larger contribution than Q^2 , and the term proportional to Y^2 is multiplies by z^2 . On the other hand, the corresponding term in (3.4) of [42] can be neglected to give a constant numerator, which make possible to proceed further. Due to the difference, we can not use the approach adapted in [42] in a reliable way except for a very special case, which we don't pursue further here.

In subsequent sections, we consider high temperature limit, called hydrodynamic limit, and low temperature limit in some details. And then we evaluate the differential equation using numerical method to see the full features of the correlation functions.

3.2.3 High Temperature Correlation Functions

For the high temperature limit, we have small parameters \mathbf{w} and \mathbf{q}^2 , which can be used as expansion parameters in equation (57). Following [34], we can derive similar results [14][16][26]. For $m = 0$ case, we calculate \mathcal{F} using incoming boundary condition at the horizon

$$\mathcal{F} = 2b^4 \pi^4 L^3 T^4 \left\{ -\frac{\mathbf{q}^2}{z_B} + (i\mathbf{w} + \mathbf{q}^2) + \mathcal{O}(\mathbf{w}^2, \mathbf{w}\mathbf{q}^2, \mathbf{q}^4) \right\}, \quad (72)$$

where we used

$$\tilde{g}_{\omega, \vec{k}}(z) = (1-z)^{i\mathbf{w}/2} \left(1 - \left(i\frac{\mathbf{w}}{2} + \mathbf{q}^2 \right) \ln \frac{1+z}{2} + \dots \right). \quad (73)$$

Note that the form of the first non-trivial contributions are the same as the results of [34] even though the differential equations are different. Yet, the physical implication seems to be more complicated. In general we can not claim to have $\mathbf{q} = 0$ for the zero momentum case $\vec{k} = 0$ because of the parameter M . The first term diverges for the strict $u_B \rightarrow 0$ limit, while the second term gives finite contributions as

$$\text{Re } \mathcal{F} = 2b^4\pi^4 L^3 T^4 \left(-\frac{M_I}{4\pi b^2 T} + \frac{2M_R\omega + \vec{k}^2}{(2\pi b T)^2} \right), \quad (74)$$

$$\text{Im } \mathcal{F} = 2b^4\pi^4 L^3 T^4 \left(\frac{M_R - 2b^2\omega}{4\pi b^2 T} + \frac{2M_I\omega}{(2\pi b T)^2} \right). \quad (75)$$

Where we put the result with $M = M_R + iM_I$ for notational simplicity.

Let us concentrate on the case $\mathbf{q} = 0$. This explicitly means that $2M_R\omega + \vec{k}^2 = 0$ and $M_I = 0$. Thus the momentum correlator has an extra contribution in imaginary part of the correlator compared to relativistic case [34]

$$\text{Re } \mathcal{F} = 0, \quad \text{Im } \mathcal{F} = 2b^4\pi^4 L^3 T^4 \frac{M_R - 2b^2\omega}{4\pi b^2 T}. \quad (76)$$

If one considers the case of zero spatial momenta $\vec{k} = 0$ and thus $M_R = 0$, we get

$$\text{Im } \mathcal{F} = -b^4\pi^3 L^3 T^3 \omega. \quad (77)$$

For the application to shear viscosity, see appendix C.

3.2.4 Low Temperature Correlation Functions

With a change of the function $\tilde{g}(z) = \sqrt{z - \frac{1}{z}} g(z)$, we get the differential equation for $g(z)$

$$g'' = (\mathbf{w}^2 F + H) g, \quad (78)$$

$$F = \frac{(1 - z^2)\mathbf{s}^2 - z^2}{z(1 - z^2)^2}, \quad H = -\frac{-3 + 6z^2 + z^4 - m^2 L^2(1 - z^2)}{4z^2(1 - z^2)^2}, \quad (79)$$

where, in the low temperature regime, $\mathbf{q}^2, \mathbf{w}^2 \gg 1$ and $\mathbf{s}^2 = \frac{\mathbf{q}^2}{\mathbf{w}^2} = \frac{2M_R\omega + \vec{k}^2}{(M_R/(2b) - b\omega)^2} \approx \mathcal{O}(1)$. Then the term proportional to \mathbf{w}^2 dominates the potential, and the solution can be found by the WKB approximation following [34]. We concentrate on the case $M_I = 0$ in this section.

The Schrödinger equation (78) has a potential, which is positive when $0 < z < z_0$ and negative when $z_0 < z < 1$, where

$$z_0 = \sqrt{\frac{\mathbf{s}^2}{1 + \mathbf{s}^2}} = \sqrt{\frac{2M_R\omega + \vec{k}^2}{(M_R/(2b) + b\omega)^2 + \vec{k}^2}}. \quad (80)$$

Thus the solution of the equation (78) decays exponentially in the interval $0 < z < z_0$ and oscillates in the interval $z_0 < z < 1$. Physically the particle has to tunnel from $z = 0$ to $z = z_0$ before it can reach the horizon $z = 1$. The imaginary part of G^R is proportional to the tunneling probability

$$\text{Im } G^R \sim \exp \left(-2|\mathbf{w}| \int_0^{z_0} dz \sqrt{F(z)} \right), \quad (81)$$

and this integral is easy to evaluate for the following two limits :

- For small \mathbf{s} ,⁵ we get $\int_0^{z_0} dz \sqrt{F(z)} = -\frac{\sqrt{2}\pi^{3/2}}{\Gamma(-\frac{1}{4})\Gamma(\frac{7}{4})} (\mathbf{s}^2)^{3/4}$, and

$$\text{Im } G^R = \exp \left(-\frac{0.556}{bT} \cdot \frac{(2M_R\omega + \vec{k}^2)^{3/4}}{(M_R/(2b) - b\omega)^{1/2}} \right). \quad (83)$$

- For large \mathbf{s} , we get $\int_0^{z_0} dz \sqrt{F(z)} = \frac{2\sqrt{\pi}\Gamma(\frac{5}{4})}{\Gamma(\frac{3}{4})} \sqrt{\mathbf{s}^2}$, and thus

$$\text{Im } G^R = \exp \left(-0.835 \frac{\sqrt{2M_R\omega + \vec{k}^2}}{bT} \right). \quad (84)$$

Thus, at low temperature, we obtain the generic behavior of the imaginary part of the correlation functions as an exponentially decaying one, $e^{-A/T}$. Specifically, the result for large \mathbf{q} , where $\text{Im } G^R \sim \exp(-\mathbf{q})$, is further confirmed by our numerical study in below.

3.3 Numerical Results

In this section we would like to present the numerical results of the correlation functions by solving the differential equation (57). For massless $m^2 = 0$ case, the series solutions of the boundary and horizon are presented in appendix B. Massive case has also similar solutions with an additional parameter $m^2 L^2$, whose behaviors are briefly explained below.

⁵One might wonder that this condition invalidates the assumption $\mathbf{q}^2, \mathbf{w}^2 \gg 1$. For $\mathbf{w} \geq \mathbf{q}$, one can evaluate the following differential equation

$$g'' = \left(\mathbf{q}^2 \tilde{F} + \tilde{H} \right) g, \quad \tilde{F} = \frac{(1 - z^2) - z^2 \tilde{\mathbf{s}}^2}{z(1 - z^2)^2}, \quad \tilde{H} = H. \quad (82)$$

where $\tilde{\mathbf{s}}^2 = 1/\mathbf{s}^2 \geq 1$. Then the term proportional to \mathbf{q}^2 dominates the potential, and the solution can be found in a similar manner.

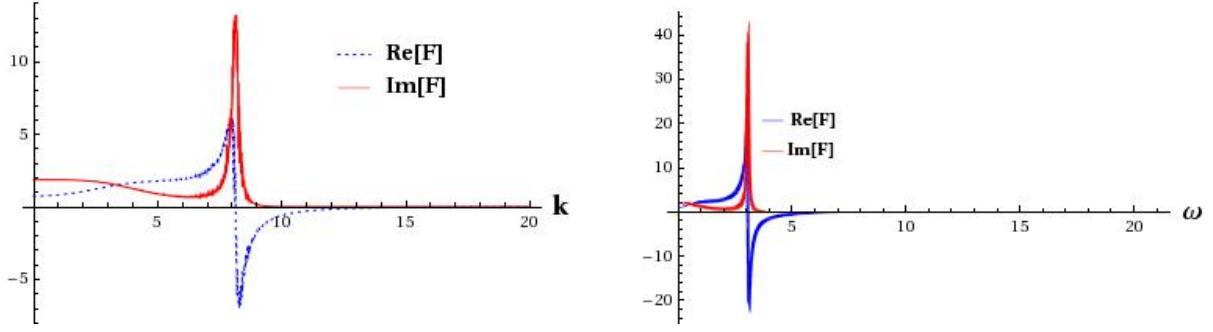


Figure 2: Real and Imaginary parts of the scalar correlation function in terms of the parameters k with $\omega = 0$ for left plot and ω with $k = 0$ for right plot for the fixed values $M = 10, b = 1$ and $T = 1$. There exist well defined peaks in imaginary part of the correlation function for both cases.

3.3.1 Description in terms of ω and k

For fixed $M = 10, b = 1$ and $T = 1$, we present plots for the real and imaginary parts of the two-point correlation function in figure 2. The left plot is for the fixed $\omega = 0$. There exist a sharp peak at finite momentum and also a much broader peak at zero momentum $k = 0$ for zero frequency. As we increase ω to the positive value, the peak moves toward to the $k = 0$ and the peak becomes bigger and narrower, while it becomes smaller and broader as we decrease ω to the negative value. The right plot is for the fixed $k = 0$. There also exists a sharp peak at finite value of ω for zero momentum. As k increase, the sharp peak moves toward negative ω and becomes smaller and broader. Thus, overall, the sharp peak becomes broader and smaller as we increase k and decrease ω .

These behaviors can be checked in the figure 3. Note that we exclude the region which gives imaginary \mathbf{q} . There is another much broader peak at $(\omega, k) = (0, 0)$, which can be identified as the point $\mathbf{q} = 0$. This peak becomes smaller and broader along the line identified by $\mathbf{q} \sim 2M\omega + k^2 = 0$. This peak can be clearly seen in an alternative description below, section 3.3.2. The above mentioned sharper peak seems to follow the broader peak line with some fixed distance, which can be described as $2M\omega + k^2 = \frac{M^2}{b^2}$. This peak is identified as the case where $\mathbf{w} = 0$. Thus we confirm that these two peaks are related to the case when each of the last two terms in (57) has vanishing contributions.

Let us comment about novel features of the scalar correlation functions for the Schrödinger geometry. First, we clearly have two peaks, of which the higher peak is distinctively clear and directly related to the unique property of the Schrödinger geometry, the isometry M and associated chemical potential $\frac{1}{2b^2}$ of the spectator direction. This, apparently, is analogous

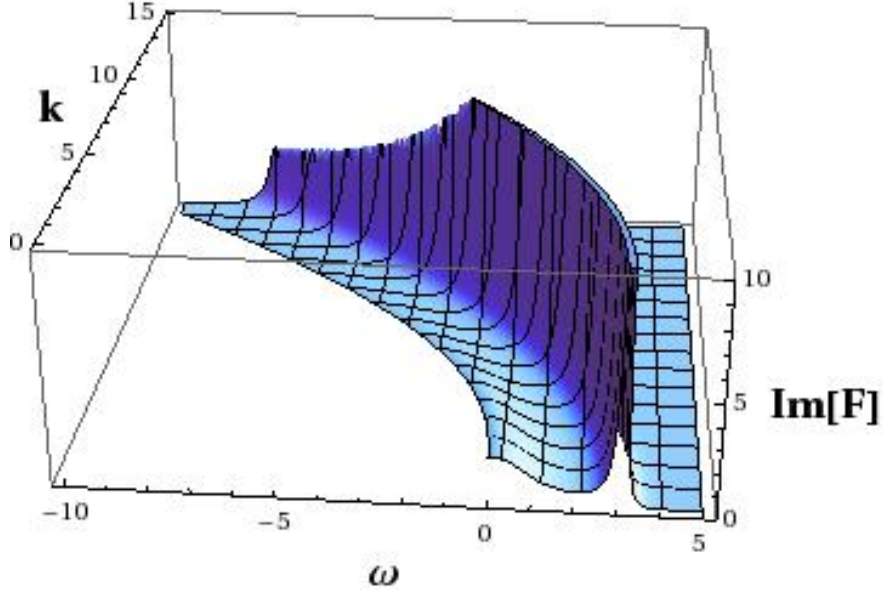


Figure 3: Imaginary part of the scalar correlation function in terms of the parameters ω, k for the fixed values $M = 10, b = 1$ and $T = 1$. They are even functions of k and we take the parameter range as $-10 \leq \omega \leq 5, 0 \leq k \leq 15$. The plots are only drawn for the parameter range $2M\omega + k^2 \geq 0$.

to the quasi-particle peak at the Fermi surface in the case of spinor. Second, the shape of our peaks in the (ω, k) space follows a curve $2M\omega + k^2 = \text{const.}$ due to the typical energy dispersion relation in non-relativistic Schrödinger type, rather than relativistic ones which would be linear in the same parameters.

3.3.2 Description in terms of \mathbf{q} and \mathbf{w}

While it is more physical to parametrize the physical properties of the correlation function in terms of ω, k , some of its properties are more transparent in terms of the parameters, \mathbf{w} and \mathbf{q} . Here we add some comments on them.

The typical shape of the correlator is depicted in figure 4. We would like to identify the corresponding peaks we observed in section 3.3.1. One of the peaks is located in $\mathbf{q} = 0$, which is matched to the broad peak located in $\omega = k = 0$. This is not exactly located at the origin but located in slightly non-zero value of the parameter $\mathbf{w} = \frac{M}{4\pi b^2 T}$, due to the non-trivial parameter M for the Schrödinger holography. The other peak is very sharp in terms of the parameter \mathbf{q} and spread out in \mathbf{w} . It is located at finite $\mathbf{q}^2 = \frac{M^2/b^2 + \vec{k}^2}{(2\pi b T)^2}$, we can identify this point near $\mathbf{w} = 0$. As we increase the value of \mathbf{w} , the peak gets smaller and

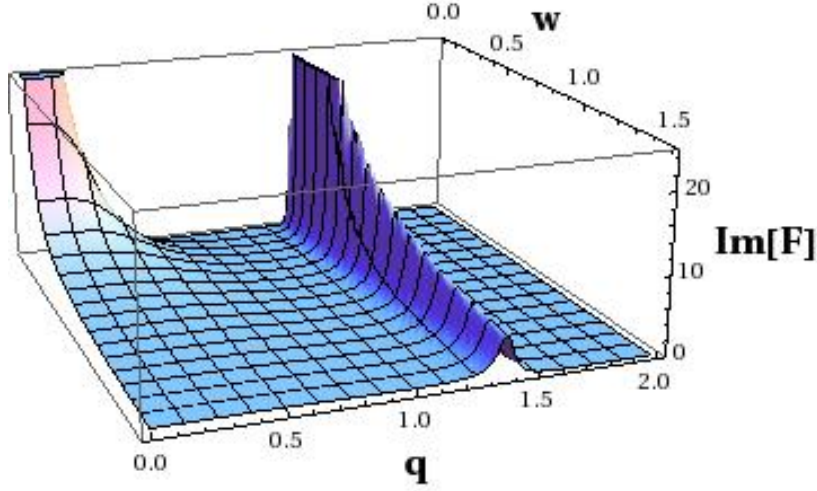


Figure 4: Imaginary part of the scalar correlation function in terms of the parameters \mathbf{w} and \mathbf{q} . There are two peaks we observed in the previous plot, figure 3.

broaden, but the peak location does not change much in \mathbf{q} .

Let us comment about the behavior of correlation function as we change the bare mass of the scalar $m^2 L^2$, which correspond to the change of the conformal dimension of the corresponding Field theory operator. For the range $-4 < m^2 L^2 < -3$, there is a single peak at $\mathbf{q} = 0$ and at small \mathbf{w} , which spread out as \mathbf{w} increases. As we increase $m^2 L^2$, the single peak moves to some positive value of \mathbf{q} without being separated from the peak at $-\mathbf{q}$. Further increase of the bare mass brings the peak to the origin around at $m^2 L^2 = 0$. For positive mass range, $m^2 L^2 > 1$, there exist two separate peaks which are similar to the zero mass case in figure 4, while the peaks are small compared to the zero mass case. With the numerical analysis, we find that massless $m^2 = 0$ case is rather special and has a well defined isolated peaks at $\mathbf{q} = 0$ and $\mathbf{w} = 0$ and spreading as we change the parameters.

Finally we would like to comment on the correlation function at large \mathbf{q} and large \mathbf{w} with $\mathbf{q} \geq \mathbf{w}$. The figure 5 represents a typical behavior in the region. We can check the exponentially decaying behavior we obtained with analytic analysis in equation (84).

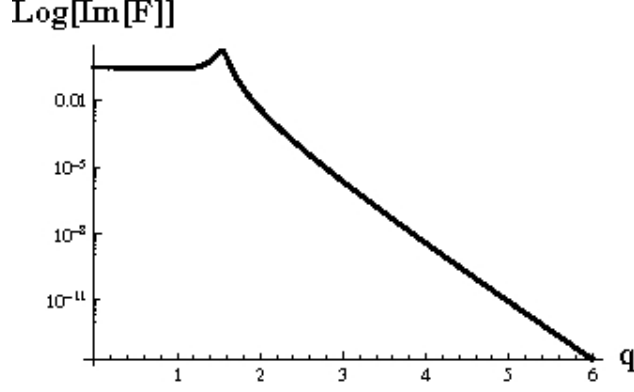


Figure 5: A typical log plot of the imaginary part for $\mathbf{w} = 3$.

3.4 Comments on Schrödinger Background

In this section we consider the aging holography from the generalized Schrödinger background [14][15][16] generated through the null Melvin twist. The action is given by

$$S = \frac{1}{16\pi G} \int d^5x \sqrt{-g} \left(R - \frac{4}{3} \partial_\mu \phi \partial^\mu \phi - \frac{1}{4} e^{-8\phi/3} F^2 - 4A^2 - 4e^{2\phi/3} (e^{2\phi} - 4) \right), \quad (85)$$

where A and F are a massive vector field and the associated field strength, and ϕ is a dilaton. The black hole geometry associated with the action was found as

$$ds^2 = r^2 k^{-2/3} \left[\left(\frac{1-h}{4b^2} - r^2 h \right) (dx^+)^2 + \frac{b^2 r_H^4}{r^4} (dx^-)^2 - (1+h) dx^+ dx^- \right] + k^{1/3} \left(r^2 d\vec{y}^2 + \frac{dr^2}{r^2 h} \right), \quad (86)$$

where

$$h = 1 - \frac{r_H^4}{r^4}, \quad k = 1 + \frac{b^2 r_H^4}{r^2}.$$

The massive vector field and dilaton also have the non-trivial configurations as

$$A = \frac{r^2}{k} \left(\frac{1+h}{2} dx^+ - \frac{b^2 r_H^4}{r^4} dx^- \right), \quad e^\phi = \frac{1}{\sqrt{k}}.$$

Following the previous section, we use the local coordinate transformation (49) to generate Aging black hole inherited from the Schrödinger background as

$$ds^2 = r^2 k^{-2/3} \left[\left(\frac{1-h}{4b^2} - r^2 h \right) (dx^+)^2 + \frac{b^2 r_H^4}{r^4} \left(dx^- + \frac{\alpha}{r} dr + \frac{\alpha}{2x^+} dx^+ \right)^2 - (1+h) dx^+ \left(dx^- + \frac{\alpha}{r} dr + \frac{\alpha}{2x^+} dx^+ \right) \right] + k^{1/3} \left(r^2 d\vec{y}^2 + \frac{dr^2}{r^2 h} \right), \quad (87)$$

with the massive vector field

$$A = \frac{r^2}{k} \left[\left(\frac{1+h}{2} - \frac{\alpha b^2 r_H^4}{2x^+ r^4} \right) dx^+ - \frac{b^2 r_H^4}{r^4} dx^- - \frac{\alpha b^2 r_H^4}{r^5} dr \right]. \quad (88)$$

We can check that the metric reduces to that of [12] when $r_h \rightarrow 0$ and also to that of [14][15][16] when $\alpha \rightarrow 0$ by construction. One can make sure that these configurations satisfy the Einstein equation.

We consider a probe free scalar on this background following the section 3.1 with the same equation of motion (51). Using the mode expansion

$$\phi(r, x^+, \vec{y}) = \int \frac{d\omega}{2\pi} \frac{d^2 k}{(2\pi)^2} \exp^{-i\vec{k} \cdot \vec{y}} T_\omega(x^+) f_{\omega, \vec{k}}(r) \phi_0(\omega, \vec{k}), \quad (89)$$

we can separate the x^+ dependent part of the differential equation with the same operator \hat{D} given in equation (55). The solution of the time dependent part is exactly the same as before, $T_\omega(x^+) = c_1 \exp^{-i\omega x^+} (x^+)^{\frac{i\alpha M}{2}}$. This is one of the main observation for the aging backgrounds compared to the Aging in light-cone.

Upon changing $z = \frac{r_h^2}{r^2}$ and $f_{\omega, \vec{k}}(z) = z^{-\frac{i\alpha M}{2}} \tilde{g}_{\omega, \vec{k}}(z)$, the z -dependent equation becomes

$$\tilde{g}'' - \frac{1+z^2}{z(1-z^2)} \tilde{g}' - \frac{(m^2 k^{1/3} + M^2)}{4z^2(1-z^2)} \tilde{g} + \frac{\mathbf{w}^2 z}{(1-z^2)^2} \tilde{g} - \frac{\mathbf{q}^2}{z(1-z^2)} \tilde{g} = 0, \quad (90)$$

where $\mathbf{w} = \frac{M/(2b^2) - \omega}{2\pi T}, \quad \mathbf{q}^2 = \frac{2M\omega + \vec{k}^2}{(2\pi bT)^2},$

with the same temperature relation $r_H = \pi bT$ and with $L = 1$ for the notational convenience. Again, this differential equation is identical to that of the Schrödinger backgrounds, confirming the general relations (17), (32) and (40) in the Schrödinger black hole backgrounds. From these observations, we argue that the local coordinate transformation (3) brings the same time dependent factor $\left(\frac{x_1^+}{x_2^+}\right)^{-\frac{i\alpha M_R}{2}}$ for $M = M_R$ given in equation (32) and $\left(\frac{x_2^+}{x_1^+}\right)^{-\frac{\alpha M_I}{2}}$ given in equation (40) to the correlation functions for the holographic aging phenomena.

This equation (90) is the same as the corresponding equation (57) of the AdS in light-cone except the following change

$$m^2 \longrightarrow m^2 k(z)^{1/3} + M^2, \quad (91)$$

which is another main observation of this section. We would like to comment about the consequences of this change without detailed investigation of this differential equation.

- In general, k depends on the radial coordinate, which is crucially different from the case of AdS in light-cone. In there, the corresponding term in equation (57) is constant

and thus it is possible to consider the case $m^2 = 0$ consistently. On the other hand, it is not possible to ignore this term for the aging Schrödinger case in general with non-zero M . This seems to be the first non-trivial evidence that there exist differences between the two different geometric realizations of Schrödinger holography.

- k is non-singular and monotonically increasing function from $k = 1$ at the boundary to $k = 1 + \pi^2 b^4 T^2$ at the horizon.
- This is the finite temperature generalization of the difference between the AdS in light-cone and the Schrödinger backgrounds, $m^2 \rightarrow m^2 + M^2$, which remains to be true at the boundary even at finite temperature. Thus we conclude that the differential equation of the Aging background is the same as that of the AdS in light-cone at the asymptotic region.

It seems that the differential equation (90) is similar to the massive case of Aging in light-cone given in (57). It remains to be seen the differences in detail with further investigations, which we postpone for the future.

4 Conclusion and Outlook

In this paper we studied the time dependent aging systems by considering their dual gravity solutions with relevant symmetry, namely aging symmetry. We mainly focused on AdS in light-cone for the field theory with Schrödinger symmetry and its aging generalizations to incorporate the aging phenomena. Using these geometries, we study the two-point correlation functions of the dual scalar fields in aging system at zero temperature as well as those in Schrödinger system at finite temperature. At zero temperature, the two-time correlation function of the dual scalar fields exhibit all the relevant features of the typical aging system. Among others, it shows that the older is the system the slower it relaxes. At finite, but low, temperature with Schrödinger isometry, the analysis of momentum space correlation function exhibits the exponentially decaying behavior as a function of the inverse temperature.

One of the important features in the Schrödinger holography and also in aging holography is the existence of the spectator direction in the bulk geometry. One usually chooses an eigenvalue M in that x^- direction, which appears as an extra free parameter in the boundary conformal field theory. In order to deal with the time dependent, open and dissipative system, it is tempting to relax the nature of this spectator or, more appropriately, internal direction and allow M to be a complex eigenvalue. Indeed, we could see that all the relevant features of the two-time correlation function in boundary aging system are revealed from the imaginary

part of M .

Another important point in this paper is the clear differences we found between Aging in light-cone and Aging backgrounds at finite temperature. They are the conformal dimensions of the scalar operators and the mass dependence of the differential equations, which can be understood simply from the differences in the effective mass, m^2 in the former and $m'^2 = m^2 k(r)^{1/3} + M^2$ for the latter. For AdS in light-cone, we evaluate two-point correlation functions in momentum space for massless scalar case, $m = 0$, with finite M using numerical method and analytic approaches for two special cases, low and high temperature limits. It seems to be possible to connect this case to read off the viscosity in AdS in light-cone with finite M for general setup, while that was not possible in Schrödinger background due to the presence of m' in the fluctuation of the gravity modes. Further systematic investigations are required to see the details, while preliminary analysis is presented in C. Thus AdS in light-cone and its generalization to aging seems to be more attractive in their physical applications at finite temperature on top of the simplicity and well-defined boundary structure.

Surely, we still need to clarify many issues to use the AdS/CFT correspondence for the time dependent field theory. Further extensive study of the aging system in this paper may shed some lights on the study in this direction. One particular example is the thermodynamic properties of time dependent backgrounds, which are readily calculated in this setup and appropriate applications can be clarified in a controllable setting due to the large isometry and simple setup [43].

Acknowledgments

We would like to thank to J. Hartong, C. Hoyos, M. Järvinen, E. Kiritsis, M. Lippert, D. Martelli, D. Minic, Y. Oz, C. Panagopoulos, J. Sonnenschein, J. Troost and D. Yamada for discussions, comments and correspondence, especially to M. Järvinen for his careful illustrations of numerical calculations. BSK is grateful to the members, especially J. Sonnenschein, of the Raymond and Beverly Sackler Faculty of Exact Sciences at Tel Aviv University for their warm hospitality during his visit. We also thank to the referee who provided several critical comments. SH is supported in part by the National Research Foundation of Korea(NRF) grant funded by the Korea government(MEST) with the grant number 2009-0074518 and the grant number 2009-0085995 and by the grant number 2005-0049409 through the Center for Quantum Spacetime(CQUeST) of Sogang University. JJ is supported by the National Research Foundation of Korea(NRF) grant funded by the Korea government(MEST) with the grant number 2009-0072755. BSK is supported through excellent grant MEXT-CT-2006-039047 and also partially supported by a European Union grant FP7-REGPOT-2008-

A High Temperature Correlator : Next Order

In section 3.2.3, we evaluate the scalar two-point correlation functions for the first non-trivial order. We evaluate the next order with the same setup. Here we summarize only the results.

$$\begin{aligned}
 \tilde{g}_{\omega, \vec{k}}(z) = & c(1-z)^{i\mathbf{w}/2} \\
 & \times \left\{ 1 + \left(i\frac{\mathbf{w}}{2} - \mathbf{q}^2 \right) \ln \frac{1+z}{2} \mathbf{q}^4 \left(\frac{5\pi^2}{24} - \ln \left[\frac{1-z}{2} \right] \ln \left[\frac{1+z}{2} \right] + \frac{1}{2} \ln[z] \ln[1+z] \right. \right. \\
 & \quad \left. \left. - \frac{1}{2} \text{PL}[2, 1-z] + \frac{1}{2} \text{PL}[2, -z] - \text{PL} \left[2, \frac{1+z}{2} \right] \right) \right. \\
 & \quad - \frac{1}{6} i\mathbf{q}^2 \mathbf{w} \left(\pi^2 - 6 \ln[2]^2 + \ln[64] \ln[1-z] \right. \\
 & \quad \quad \left. - 6 \ln \left[\frac{1-z}{2} \right] \ln[1+z] - 6 \text{PL} \left[2, \frac{1+z}{2} \right] \right) \\
 & \quad + \frac{1}{24} \mathbf{w}^2 \left(-2\pi^2 + 15 \ln[2]^2 + 12 \ln[1-z] \ln \left[\frac{1+z}{2} \right] \right. \\
 & \quad \quad \left. \left. + 3 \ln[1+z] (-2 \ln[8] + \ln[1+z]) + 12 \text{PL} \left[2, \frac{1+z}{2} \right] \right) \right\} , \quad (92)
 \end{aligned}$$

where

$$c = \frac{24}{\pi^2 (\mathbf{q}^2 - i\mathbf{w})^2 + 3(8 + \ln[2])(-4\mathbf{q}^4 \ln[2] + \mathbf{q}^2(8 + 4i\mathbf{w} \ln[2]) + \mathbf{w}(-4i + \mathbf{w} \ln[8]))} . \quad (93)$$

Where PL is PolyLog. Following the standard prescription, we normalize the wave solution to be unity at $z = 0$ and use the incoming boundary condition at $z = 1$.

From the first two non-trivial orders of the expansion, we can calculate the momentum correlator as

$$\frac{\mathcal{F}}{2b^4\pi^4 L^3 T^4} = -\frac{\mathbf{q}^2}{z_B} - i\mathbf{w} + \mathbf{q}^2 + \mathbf{q}^4 + (2i\mathbf{w}\mathbf{q}^2 + \mathbf{w}^2) \ln[2] - \mathbf{q}^4 \ln[4z_B] + \dots . \quad (94)$$

Note that this is similar to the relativistic results [34] if we identify the parameters our \mathbf{w} and \mathbf{q} as relativistic frequency and momentum, respectively. But the physical meaning of these two parameters are very different and we develop several imaginary contributions by introducing complex M as we explained in section 3.2.3. In particular, there is another non-trivial contribution $\mathbf{w}^2 \ln[2]$ in the next order in addition to $-i\mathbf{w}$ even in the case $\mathbf{q} = 0$.

B Series Solutions with $m = 0$

Here we solve the differential equation (57) at the boundary and at the horizon with appropriate expansions in each regions. These series solutions are used in the section 3.3. It is also interesting to consider general cases with non-zero mass m^2 , we would like to concentrate on $m = 0$ in the differential equation (57). These series solutions are used to evaluate the radial part \mathcal{F} of the correlator as

$$\mathcal{F} = \frac{b^4 \pi^4 L^5 T^4}{2z^3} \left(\frac{\tilde{g}_{\omega, \vec{k}}(z)}{\tilde{g}_{\omega, \vec{k}}(z_B)} \right)^* \frac{4z^2 h_z}{L^2} \partial_z \left(\frac{\tilde{g}_{\omega, \vec{k}}(z)}{\tilde{g}_{\omega, \vec{k}}(z_B)} \right) \Big|_{z \rightarrow z_B}. \quad (95)$$

At the boundary, we found a series solution upto 6th order of the expansion as

$$\tilde{g}_B = A \left(\sum_{n=0}^5 a_n z^n + \sum_{n=2}^5 b_n z^n \ln z \right) + B \left(\sum_{n=0}^5 c_n z^{n+2} \right). \quad (96)$$

We explicitly list here only the first four terms as

$$\begin{aligned} a_0 &= 1, & a_1 &= -\mathbf{q}^2, & a_2 &= 0, & a_3 &= \frac{1}{9} (-3 \mathbf{q}^2 + 2 \mathbf{q}^6 - 3 \mathbf{w}^2), \\ b_2 &= -\frac{1}{2} \mathbf{q}^4, & b_3 &= -\frac{1}{6} \mathbf{q}^6, \\ c_0 &= 1, & c_1 &= \frac{\mathbf{q}^2}{3}, & c_2 &= \frac{1}{24} (12 + \mathbf{q}^4), & c_3 &= \frac{1}{360} (84 \mathbf{q}^2 + \mathbf{q}^6 - 24 \mathbf{w}^2). \end{aligned} \quad (97)$$

This solution has two independent parameters, A and B , which can be fixed by the solving the differential equation at the horizon using incoming boundary condition and by interpolating the solution to the boundary.

At the horizon we have a similar series solution upto 6th order of the expansion

$$\tilde{g}_H = (1 - z)^{\frac{i\mathbf{w}}{2}} \left(\sum_{n=0}^5 d_n (1 - z)^n \right), \quad (98)$$

with incoming boundary condition at the horizon as explained in the main body. The first four coefficients are

$$\begin{aligned} d_0 &= 1, & d_1 &= \frac{2i\mathbf{q}^2 + \mathbf{w}}{4i - 4\mathbf{w}}, \\ d_2 &= -\frac{4\mathbf{q}^4 + \mathbf{q}^2(8 + 8i\mathbf{w}) + \mathbf{w}(-4i + 6\mathbf{w} + i\mathbf{w}^2)}{32(-2 - 3i\mathbf{w} + \mathbf{w}^2)}, \\ d_3 &= -\frac{8\mathbf{q}^6 + 12\mathbf{q}^4(8 + 5i\mathbf{w}) + 6\mathbf{q}^2(2 + i\mathbf{w})(8 + \mathbf{w}(8i + \mathbf{w}))}{384(6 - i\mathbf{w}(-11 + \mathbf{w}(-6i + \mathbf{w})))} \\ &\quad - \frac{\mathbf{w}(-48i + \mathbf{w}(108 + (54i - 5\mathbf{w})\mathbf{w}))}{384(6 - i\mathbf{w}(-11 + \mathbf{w}(-6i + \mathbf{w})))}. \end{aligned} \quad (99)$$

These two solutions, near boundary and near horizon solutions, can be connected numerically. And the two-point correlation function is given by

$$\frac{\mathcal{F}}{4b^4\pi^4 L^3 T^4} = \frac{B}{A} \quad (100)$$

in terms of various parameters we are interested in.

C Shear Viscosity

The finite temperature hydrodynamic correlation functions for the off-diagonal component of the energy-momentum tensor $\langle T_{y_1}^{y_2} T_{y_1}^{y_2} \rangle$ were evaluated for the Schrödinger background in [14][16], while that of the AdS in light-cone was done in [26]. It is interesting to recall that the viscosity-entropy ratio for the strongly coupled non-relativistic plasma also satisfies the universal bound, $\frac{\eta}{s} = \frac{1}{4\pi}$ [14][16][26] for $\omega/T \ll 1$ with vanishing parameters including M as confirmed in section 3.2.3. If we demand $M = \vec{k} = 0$, the calculations are simple and effectively identical to those with the wave equation for a massless scalar field of AdS₅ black hole.

Let us revisit the earlier treatments to evaluate the shear viscosity concentrating on Schrödinger geometry, which essentially used the scalar correlation functions, as advertised in [44]. While it is straightforward to identify the correlation functions of the energy-momentum tensor to those of scalar operators for the relativistic case with the vanishing spatial momenta, there exist subtleties due to the internal direction in the non-relativistic Schrödinger case. It is argued in [14] that $M = 0$ is required to evaluate the shear viscosity in the Schrödinger background. The scalar operator has the conformal dimension $\Delta = 2 + \sqrt{4 + L^2 m^2 + M^2}$ in the Schrödinger backgrounds, while the gravity modes have the conformal dimension $\Delta = 4$. Thus it is required to put $M = m = 0$ to calculate the shear viscosity using the scalar operator, and thus restricted to the sector, $M = 0$.

The story is different for the AdS in light-cone. As we mentioned in several places, we concentrate on the fixed sector of M and we would like to consider the fluctuation equation of the off-diagonal component as in [14]

$$\delta g_{y_1}^{y_2} = e^{-i\omega x^+ + iM x^-} \Phi(r) , \quad (101)$$

which satisfy the following differential equation

$$\Phi'' + \frac{4+h}{rh} \Phi' + \frac{(M^2 + 4b^4\omega^2)(1-h) - 4b^2 M\omega(1+h)}{4b^2 r^4 h^2} \Phi = 0 . \quad (102)$$

Thus we are supposed to solve this differential equation directly to get the correlation functions related to the metric fluctuations. This equation is nothing but the scalar differential

equation given in (57) with $m = 0$, expressed in the z -coordinate. Now a crucial difference comes into play. Note that the conformal dimension of a scalar operator is given by $\Delta = 2 + \sqrt{4 + L^2 m^2}$. Thus we can just restrict ourselves to the case $m = 0$, which is already taken care of in (57). This made it possible to read off the viscosity, for general sector M , readily from the boundary two-point correlation of the scalar fields using the equation (102). This would be regarded as a crucial difference between the AdS in light-cone and Schrödinger backgrounds in the finite temperature case. We defer the systematic analysis for finite M with full generality to the future.

For $m = 0$, being required by the conformal dimension of the energy momentum tensor, and $M = 0$, being required by the condition $\mathbf{q} = 0$ (this restriction would be lifted for general setup), we can read off the shear viscosity from the equation (77)

$$\eta = \frac{b^4 \pi^3 L^3 T^3}{16G} \quad \rightarrow \quad \frac{\eta}{s} = \frac{1}{4\pi}, \quad (103)$$

where we use the entropy formula from [26] and take into account the factor K in front of the action (9). This is the advertised entropy-viscosity ratio of the strongly-coupled non-relativistic fluid advertised in [14][16][26]. The result is the same as the relativistic counterpart for $M = 0$.

References

- [1] J. M. Maldacena, "The large N limit of superconformal field theories and super-gravity," Adv. Theor. Math. Phys. **2**, 231 (1998) [Int. J. Theor. Phys. **38**, 1113 (1999)] [arXiv:hep-th/9711200]; S. S. Gubser, I. R. Klebanov and A. M. Polyakov, "Gauge theory correlators from non-critical string theory," Phys. Lett. B **428**, 105 (1998) [arXiv:hep-th/9802109]; E. Witten, "Anti-de Sitter space and holography," Adv. Theor. Math. Phys. **2**, 253 (1998) [arXiv:hep-th/9802150].
- [2] O. Aharony, S. S. Gubser, J. M. Maldacena, H. Ooguri and Y. Oz, "Large N field theories, string theory and gravity," Phys. Rept. **323**, 183 (2000) [arXiv:hep-th/9905111].
- [3] D. T. Son, "Toward an AdS/cold atoms correspondence: a geometric realization of the Schroedinger symmetry," Phys. Rev. D **78**, 046003 (2008) [arXiv:0804.3972 [hep-th]].
- [4] K. Balasubramanian and J. McGreevy, "Gravity duals for non-relativistic CFTs," Phys. Rev. Lett. **101**, 061601 (2008) [arXiv:0804.4053 [hep-th]].
- [5] W. D. Goldberger, "AdS/CFT duality for non-relativistic field theory," JHEP **0903**, 069 (2009) [arXiv:0806.2867 [hep-th]].

- [6] J. L. F. Barbon and C. A. Fuertes, “On the spectrum of nonrelativistic AdS/CFT,” JHEP **0809**, 030 (2008) [arXiv:0806.3244 [hep-th]].
- [7] S. Kachru, X. Liu and M. Mulligan, “Gravity Duals of Lifshitz-like Fixed Points,” Phys. Rev. D **78**, 106005 (2008) [arXiv:0808.1725 [hep-th]].
- [8] P. Hořava, “Quantum Gravity at a Lifshitz Point,” Phys. Rev. D **79**, 084008 (2009) [arXiv:0901.3775 [hep-th]].
- [9] L. F. Cugliandolo, “Dynamics of glassy system,” arXiv:cond-mat/0210312.
- [10] M. Henkel and M. Pleimling, “Non-equilibrium phase transitions,” arXiv:cond-mat/0703466.
- [11] D. Minic and M. Pleimling, “Non-Relativistic AdS/CFT and Aging/Gravity Duality,” Phys. Rev. E **78**, 061108 (2008) [arXiv:0807.3665].
- [12] J. I. Jottar, R. G. Leigh, D. Minic and L. A. Pando Zayas, “Aging and Holography,” JHEP **1011**, 034 (2010) [arXiv:1004.3752 [hep-th]].
- [13] Y. Nakayama, “Universal time dependent deformations of Schrodinger geometry,” JHEP **1004**, 102 (2010) [arXiv:1002.0615 [hep-th]].
- [14] C. P. Herzog, M. Rangamani and S. F. Ross, ”Heating up Galilean holography,” JHEP **0811**, 080 (2008) [arXiv:0807.1099 [hep-th]].
- [15] J. Maldacena, D. Martelli and Y. Tachikawa, ”Comments on string theory backgrounds with non-relativistic conformal symmetry,” JHEP **0810**, 072 (2008) [arXiv:0807.1100 [hep-th]].
- [16] A. Adams, K. Balasubramanian and J. McGreevy, ”Hot Spacetimes for Cold Atoms,” JHEP **0811**, 059 (2008) [arXiv:0807.1111 [hep-th]].
- [17] D. Yamada, ”Thermodynamics of Black Holes in Schroedinger Space,” Class. Quant. Grav. **26**, 075006 (2009) [arXiv:0809.4928 [hep-th]].
- [18] M. Ammon, C. Hoyos, A. O’Bannon and J. M. S. Wu, “Holographic Flavor Transport in Schrodinger Spacetime,” JHEP **1006**, 012 (2010) [arXiv:1003.5913 [hep-th]].
- [19] E. G. Gimon, A. Hashimoto, V. E. Hubeny, O. Lunin and M. Rangamani, “Black strings in asymptotically plane wave geometries,” JHEP **0308**, 035 (2003) [arXiv:hep-th/0306131].

- [20] M. Alishahiha and O. J. Ganor, “Twisted backgrounds, PP waves and nonlocal field theories,” JHEP **0303**, 006 (2003) [arXiv:hep-th/0301080].
- [21] S. A. Hartnoll and K. Yoshida, “Families of IIB duals for nonrelativistic CFTs,” JHEP **0812**, 071 (2008) [arXiv:0810.0298 [hep-th]].
- [22] C. Duval, M. Hassaine and P. A. Horvathy, “The Geometry of Schrodinger symmetry in gravity background/non-relativistic CFT,” Annals Phys. **324**, 1158 (2009) [arXiv:0809.3128 [hep-th]].
- [23] L. Mazzucato, Y. Oz and S. Theisen, “Non-relativistic Branes,” JHEP **0904**, 073 (2009) [arXiv:0810.3673 [hep-th]].
- [24] J. Jeong, H. C. Kim, S. Lee, E. O Colgain and H. Yavartanoo, “Schrodinger invariant solutions of M-theory with Enhanced Supersymmetry,” JHEP **1003**, 034 (2010) [arXiv:0911.5281 [hep-th]].
- [25] H. C. Kim, S. Kim, K. Lee and J. Park, “Emergent Schrodinger geometries from mass-deformed CFT,” arXiv:1106.4309 [hep-th].
- [26] B. S. Kim and D. Yamada, “Properties of Schroedinger Black Holes from AdS Space,” JHEP **1107**, 120 (2011) [arXiv:1008.3286 [hep-th]].
- [27] B. S. Kim, E. Kiritsis and C. Panagopoulos, ”Strange metal behavior from the Light-Cone AdS Black Hole,” arXiv:1012.3464 [cond-mat.str-el]
- [28] M. Guica, K. Skenderis, M. Taylor and B. C. van Rees, “Holography for Schrodinger backgrounds,” JHEP **1102**, 056 (2011) [arXiv:1008.1991 [hep-th]].
- [29] K. Balasubramanian and J. McGreevy, “The Particle number in Galilean holography,” JHEP **1101**, 137 (2011) [arXiv:1007.2184 [hep-th]].
- [30] V. Balasubramanian and P. Kraus, ”A stress tensor for anti-de Sitter gravity,” Commun. Math. Phys. **208**, 413 (1999) [arXiv:hep-th/9902121].
- [31] S. de Haro, S. N. Solodukhin and K. Skenderis, “Holographic reconstruction of space-time and renormalization in the AdS/CFT correspondence,” Commun. Math. Phys. **217**, 595 (2001) [arXiv:hep-th/0002230].
- [32] S. F. Ross and O. Saremi, “Holographic stress tensor for non-relativistic theories,” JHEP **0909**, 009 (2009) [arXiv:0907.1846 [hep-th]].
- [33] P. Hořava and C. M. Melby-Thompson, ”Anisotropic Conformal Infinity,” Gen. Rel. Grav. **43** (2011) 1391 [arXiv:0909.3841 [hep-th]].

- [34] D. T. Son and A. O. Starinets, “Minkowski-space correlators in AdS/CFT correspondence: Recipe and applications,” *JHEP* **0209**, 042 (2002) [arXiv:hep-th/0205051].
- [35] D. T. Son and A. O. Starinets, “Viscosity, Black Holes, and Quantum Field Theory,” *Ann. Rev. Nucl. Part. Sci.* **57**, 95 (2007) [arXiv:0704.0240 [hep-th]].
- [36] K. Skenderis and B. C. van Rees, “Real-time gauge/gravity duality,” *Phys. Rev. Lett.* **101**, 081601 (2008) [arXiv:0805.0150 [hep-th]].
- [37] K. Skenderis and B. C. van Rees, “Real-time gauge/gravity duality: Prescription, Renormalization and Examples,” *JHEP* **0905**, 085 (2009) [arXiv:0812.2909 [hep-th]].
- [38] M. Henkel, “Phenomenology of local scale invariance: From conformal invariance to dynamical scaling,” *Nucl. Phys. B* **641**, 405 (2002) [arXiv:hep-th/0205256].
- [39] O. J. Ganor and S. Sethi, “New perspectives on Yang-Mills theories with sixteen supersymmetries,” *JHEP* **9801**, 007 (1998) [arXiv:hep-th/9712071].
- [40] A. Kapustin and S. Sethi, “The Higgs branch of impurity theories,” *Adv. Theor. Math. Phys.* **2**, 571 (1998) [arXiv:hep-th/9804027].
- [41] S. Hyun, J. Jeong and B. S. Kim, to appear.
- [42] G. Policastro and A. Starinets, “On the absorption by near-extremal black branes,” *Nucl. Phys. B* **610**, 117 (2001) [arXiv:hep-th/0104065].
- [43] S. Hyun, J. Jeong and B. S. Kim, work in progress.
- [44] P. Kovtun, D. T. Son, A. O. Starinets, “Holography and hydrodynamics: Diffusion on stretched horizons,” *JHEP* **0310**, 064 (2003). [arXiv:hep-th/0309213 [hep-th]].